Molecular Pharmacology Fast Forward. Published on February 28, 2005 as doi:10.1124/mol.104.009423
This article has not been copyedited and formatted. The final version may differ from this version.

Title page.

Identification and characterisation of PDE4A11, a novel, widely expressed long isoform encoded by the human *PDE4A* cyclic AMP phosphodiesterase gene†.

by

Derek A. Wallace, Lee Ann Johnston, Elaine Huston, Douglas MacMaster, Thomas M. Houslay, York-Fong Cheung, Lachlan Campbell, Jenni E Millen, Robin A Smith, Irene Gall, Richard G. Knowles, Michael Sullivan & Miles D. Houslay¶

Molecular Pharmacology Group, Division of Biochemistry and Molecular Biology. Institute of Biomedical & Life Sciences, Wolfson Building, University Avenue, University of Glasgow, Glasgow G12 8QQ, Scotland, U.K (DAW, LAJ, EH, DM, TMH, YFC, LC, JEM, IG, MDH).

GSK, Respiratory Pharmacology, Gunnels Wood Road, Stevenage, Herts, SG1 2NY, UK (RAS, RGK)

Astra Charnwood, Bakewell Road, Loughborough, LE11 0RH, UK (MS)

Molecular Pharmacology Fast Forward. Published on February 28, 2005 as DOI: 10.1124/mol.104.009423
This article has not been copyedited and formatted. The final version may differ from this version.

Running title page.

running title : Cloning and expression of PDE4A11

¶ Corresponding author.
Miles D Houslay, PhD
Molecular Pharmacology Group,
Division of Biochemistry and Molecular Biology.
Institute of Biomedical & Life Sciences,
Wolfson Building, University Avenue,
University of Glasgow,
Glasgow G12 8QQ,
Scotland, U.K

Email M.Houslay@bio.gla.ac.uk,
phone +44-(0)141-330-5803,
fax +44-(0)141-330-4365

text pages total is 40
tables: 3
figures: 10
references: 40
abstract words: 247
Introduction words:- 354
Discussion words:- 1489

Molecular Pharmacology Fast Forward. Published on February 28, 2005 as DOI: 10.1124/mol.104.009423
This article has not been copyedited and formatted. The final version may differ from this version.

Abstract

PDE4A11 is a novel cAMP specific phosphodiesterase that is conserved in man, mouse, rat, pig and bat. Exon-1^{4A11} encodes its unique, 81 amino acid N-terminal region. RT-PCR, done across the splice junction, plus identification of ESTs, identifies PDE4A11 as a long isoform, possessing UCR1 and UCR2 regulatory domains. Transcript analysis shows that PDE4A11 is widely expressed compared to PDE4A10 and PDE4A4B long isoforms. Truncation analysis identifies a putative promoter in a 250bp region located immediately upstream of the start site in Exon-1^{4A11}. Recombinant PDE4A11, expressed in COS7 cells, is a 126kDa protein localised predominantly around the nucleus and in membrane ruffles. PDE4A11 exhibits a Km for cAMP hydrolysis of 4μM with similar relative Vmax to PDE4A10 and PDE4A4B. PDE4A11 is dose-dependently inhibited by rolipram, Ro20-1724, cilomilast, roflumilast and denbufylline with IC_{50} values of 0.7, 0.9, 0.03, 0.004 and 0.3 μM, respectively. Soluble and particulate PDE4A11 exhibit distinct rates of thermal inactivation (55˚C; T(0.5) = 2.5 and 4.4 min, respectively). Elevating cAMP levels in COS7 cells activates PDE4A11 concomitant with its phosphorylation at Ser119 by protein kinase A. PDE4A11 differs from PDE4A4 in sensitivity to cleavage by caspase-3, interaction with LYN SH3 domain, redistribution upon chronic rolipram challenge and sensitivity to certain PDE4 inhibitors. PDE4A11, PDE4A10 and PDE4A4 all can interact with βarrestin. PDE4A11 is a novel, widely expressed long isoform that is activated by PKA phosphorylation and shows a distinct intracellular localisation, indicating that it may contribute to compartmentalised cAMP signalling in cells where it is expressed.

Molecular Pharmacology Fast Forward. Published on February 28, 2005 as DOI: 10.1124/mol.104.009423
This article has not been copyedited and formatted. The final version may differ from this version.

Introduction

The inactivation of the key second messenger cAMP is achieved through the action of a large multi-gene family of cyclic nucleotide phosphodiesterases (see e.g. (Beavo and Brunton, 2002; Maurice et al., 2003)). Of these, the PDE4 cAMP specific phosphodiesterase family has attracted considerable attention (Conti et al., 2003; Houslay and Adams, 2003). One reason for this is that PDE4 selective inhibitors act as potent anti-inflammatory agents and are currently being developed to treat various inflammatory diseases, such as chronic obstructive pulmonary disease (COPD), asthma and Crohn's Disease (see e.g. (Burnouf and Pruniaux, 2002; Giembycz, 2002). The validity of such approaches has been strongly supported by targeted gene inactivation studies (Conti et al., 2003; Mehats et al., 2003). Additionally, PDE4 isoforms appear to be targeted to interact with specific proteins / lipids in cells (Houslay and Adams, 2003) and, in so doing, play a pivotal role in underpinning the compartmentalisation of cAMP signalling (Mongillo et al., 2004).

Four genes (PDE4A, PDE4B, PDE4C, PDE4D) generate a large family of PDE4 isoforms through the use of distinct promoters and alternative mRNA splicing (Conti et al., 2003; Houslay and Adams, 2003). Their unique N-terminal regions, each of which is encoded by a specific 5' exon, thus define individual PDE4 isoforms. PDE4 isoforms are then further subcategorised into either long forms, which possess the regulatory UCR1 and UCR2 modules, or short isoforms, which lack UCR1 or super-short isoforms, which lack UCR1 and have a truncated UCR2 (Conti et al., 2003; Houslay and Adams, 2003). The UCR1 module confers susceptibility to activation by PKA-mediated phosphorylation (Hoffmann et al., 1998; MacKenzie et al., 2002; Sette and Conti, 1996), which is thought to provide part of the cellular machinery allowing desensitization to cAMP signalling by accelerating cAMP degradation (Conti et al., 2003). Also, the UCR1/2 modules serve to orchestrate the functional outcome of ERK phosphorylation of the PDE4 catalytic unit (MacKenzie et al., 2000). This is observed for the PDE4B, PDE4C and PDE4D isoforms, but not PDE4A isoforms whose catalytic unit lacks the consensus site for ERK phosphorylation (Baillie et al., 2000).

Molecular Pharmacology Fast Forward. Published on February 28, 2005 as DOI: 10.1124/mol.104.009423
This article has not been copyedited and formatted. The final version may differ from this version.

To date the human *PDE4A* gene has been shown to encode a short form, called PDE4A1 (Sullivan et al., 1998), the long isoforms PDE4A4B (Bolger et al., 1993) and PDE4A10 (Rena et al., 2001) and a catalytically inactive N- and C-terminally truncated PDE4A7 (Johnston et al., 2004). Interestingly, the PDE4A4B long isoform appears to be up-regulated in macrophages from smokers with COPD (Barber et al., 2004) and PDE4A10 has been shown to be up-regulated upon differentiation of monocytes to macrophages (Shepherd et al., 2004). Here we describe the identification and characterisation of a novel, widely expressed PDE4A long isoform, which we call PDE4A11.

Materials and Methods

[^{3}H]-cyclic AMP and ECL reagent were from Amersham International (Amersham, UK). Dithiothreitol, *N*--{1-(2,3-Dioleoyloxy)propyl}-*N,N,N*,-trimethylammonium methylsulfate (DOTAP) and protease inhibitor tablets were obtained from Boehringer Mannheim (Mannheim, Germany). Bradford reagent was from Bio-Rad (Herts, UK). All other materials were from Sigma (Poole, UK).

SDS/PAGE and Western Blotting

4-12% acrylamide gels were used and the samples boiled for 5min after being resuspended in SDS sample buffer. Gels were run at 100V/gel for 1-2h with cooling. For detection of transfected PDE by western blotting, 2-50µg protein samples were separated by SDS-PAGE and then transferred to nitrocellulose before being immunoblotted using the indicated specific antisera. Labelled bands were identified using peroxidase linked to anti-rabbit IgG and the Amersham ECL western blotting kit was used as a visualization protocol. We used polyclonal antisera able to detect all active human PDE4A isoforms as described previously (Huston et al., 1996). This was raised against the extreme C-terminal region that is unique to the PDE4A sub-family and which is found in all known active PDE4 isoforms. We also used a polyclonal antiserum (PS54-UCR1-A1) able to detect the (protein kinase A) phospho-serine form of the Arg-Arg-

Molecular Pharmacology Fast Forward. Published on February 28, 2005 as DOI: 10.1124/mol.104.009423
This article has not been copyedited and formatted. The final version may differ from this version.

Glu-Ser-Phe motif found in the conserved UCR1 region of all long isoforms (MacKenzie et al., 2002).

Bio-informatics analyses

The 38 kb region of the human PDE4A gene locus and the 33 kb region of the murine PDE4A gene locus were analysed by PROSCAN (http://bimas.dcrt.nih.gov/molbio/proscan/), a PolII promoter prediction program, the GRAIL CpG prediction program (http://compbio.ornl.gov/grailexp/) and the GENSCAN exon prediction program (http://genes.mit.edu/GENSCAN.html). Putative transcription factor binding sites within the PDE4A11 promoter were identified using both the on-line software resource, TESS at http://www.cbil.upenn.edu/tess and also TRANSFAC software available at http://motif.genome.ad.jp/.

Constructs

The ORF encoding the 860 amino acids of human PDE4A11 (GenBank AY618547), as predicted from the HSPDE4A genomic sequence and cDNA fragments, was engineered for expression in pcDNA3, as done before by us for PDE4A10 (Rena et al., 2001). The Ser119Ala mutation of PDE4A11 was generated using the QuikChange Site-Directed Mutagenesis Kit (Stratagene, UK) according to the manufacturers instructions. The presence of the appropriate mutation was confirmed by DNA sequencing as done before by us (Hoffmann et al., 1998; MacKenzie et al., 2002).

The expression plasmids encoding PDE4A4B and PDE4A10 isoforms have been described in detail previously by us (Huston et al., 1996; Rena et al., 2001; Sullivan et al., 1998).

A plasmid encoding PDE4A4B with eGFP fused to its C-terminus was used as described before by us (Terry et al., 2003). A plasmid encoding PDE4A11 with eGFP fused at its C-terminus, for expression in mammalian cells, was generated using the ORF of PDE4A11 in pcDNA3 as a template for PCR (Qiagen HotStarTaq DNA Polymerase) in order to incorporate a HindIII site at 5' end and a BamH1 site at 3' end (no STOP to read through GFP). The PCR product was run on Low Melting Point Agarose gel, band cut out and purified (QIAquik Gel EXtraction Kit from Qiagen). This was then ligated (Roche Rapid Ligation Kit) into HindIII/BamHI cut pEGFPN1 (Clontech). A plasmid

Molecular Pharmacology Fast Forward. Published on February 28, 2005 as DOI: 10.1124/mol.104.009423
This article has not been copyedited and formatted. The final version may differ from this version.

encoding PDE4A10 with eGFP fused at its C-terminus for expression in mammalian cells was similarly generated. All constructs were confirmed by sequencing.

A putative PDE4A11 promoter construct was formed by cloning a 1kb fragment immediately upstream of the ATG start for PDE4A11 into the SmaI site of pGL3-Basic (Promega) to generate p4A11-Luc. Primers corresponding with bases some 750, 500 and 250 bp into the 1kb PDE4A11 promoter construct were designed. Deletions were PCR amplified from the 1kB construct using Platinum Pfx polymerase with PCR conditions of 94^{o}C for 2 minutes and cycle conditions of 94^{o}C for 15 seconds, 55^{o}C for 30 seconds and 68^{o}C for 1 min> This was repeated up to 45, as indciated. The fragments were then cloned using the TOPO TA Cloning Kit (InVitrogen) according to the manufacturer's protocol. Deletions with the correct orientation were selected using restriction digests. DNA was extracted using the Qiagen Spin Mini Prep kit according to the manufacturer protocol. The constructs are referred to by the number of bases that they contain immediately 5' to the ATG start of PDE4A11 in exon1^{4A11}. In making these deletions the reverse primer used was GGCCGCGGGGCGGCCCCGCCTCGGCGGGCG and the forward primers were GATGGGGAGCTCTGGAGGAATTTTGGGACA (deletion to 750 bp), GAGAGTGCCCTAGGGTTTATGAGGGTGTCT (deletion to 500bp) and GGCGATTGTGAGGACATTAGAGCCAACGCG (deletion to 250bp).

A PDE4A10 promoter construct consisting of 1kb of sequence upstream from exon-1^{4A1}0 and a PDE4A4B promoter construct consisting of 1kb of sequence upstream from exon-1^{4A4B}, each fused to a luciferase reporter, was as described before by us (Rena et al., 2001).

TaqMan mRNA profiles

Leukocytes were isolated from blood samples donated by volunteers at GSK, Stevenage, UK. Bronchial epithelial and smooth muscle primary cells were obtained from Clonetics, USA. Poly A^{+} RNA was prepared by the PolyATract method according to manufacturer's instructions (Promega, USA) from the indicated cells of three different individuals. It was then pooled, reverse transcribed and analysed by TaqMan quantitative PCR (Chapman et al., 2000). Briefly, 0.5 – 1 μg of poly A+ RNA was reverse transcribed using random priming to produce cDNA. Samples were diluted so that wells contained

Molecular Pharmacology Fast Forward. Published on February 28, 2005 as DOI: 10.1124/mol.104.009423
This article has not been copyedited and formatted. The final version may differ from this version.

cDNA produced from 1ng poly A+ RNA. TaqMan quantitative PCR (Applied Biosystems, Warrington, UK) was used to assess the level of each gene. A scale factor normalisation method was used to normalise expression against those of three housekeeping genes (cyclophilin, β-actin and GAPDH).

Gene-specific reagents for PDE4A4B were, forward primer GGTGTAGGTTGGAAGGGCCA, reverse primer CAGAGACAGGCTCCTTTCCG, TaqMan probe ATGGAACCCCCGACCGTCCCCT. Gene-specific reagents for PDE4A10 were, forward primer CCCTGCCCTGGCACT, reverse primer ACAGATCTGCCCGGAGGGT, TaqMan probe CACTTCCCCTTCAGCGATGAGGACACC. Gene-specific reagents for PDE4A11 were, forward primer GGCTGAGGACGAGGCGTT, reverse primer GAAGGCGTCTGCGGAAAGTT, TaqMan probe CTCCTCGCCCGTCTTCTTCGCCAG; HOUSEKEEPER GAPDH forward primer CAAGGTCATCCATGACAACTTTG, reverse primer GGCCATCCACAGTCTTCTGG, TaqMan probe ACCACAGTCCATGCCATCACTGCCA.

RT-PCR analyses.

Amplification of PDE4A11 fragments was carried out using intron-spanning primers. This was done from 2 μg mRNA using HotStar Taq DNA Polymerase (Qiagen, Crawley, UK) and PCR conditions 50^{o}C for 30 minutes, 94^{o}C for 15 minutes and 35 cycles of 94^{o}C for 1 minute, 50^{o}C for 1 minute and 72^{o}C for 1 minute. Final extension was carried out at 72^{o}C for 10 minutes and the RT-PCR product was visualized by electrophoresis using a 1.2% agarose gel containing ethidium bromide at a final concentration of 0.5 μg/ml. The generic PDE4A fragments were amplified using the sense primer ATGCAGACCTATCGCTCTGTCAGC and the anti-sense primer ACCATCGTGTCCACAGGGATGC to detect a product of 506 bp encoding the PDE4A common region, from UCR2 into the catalytic unit. The PDE4A11 specific fragments were generated using the sense primer ATGGCGCGGCCGCGCGGCCTAGGCC and the anti-sense primers CGGACGCTCCGGAGGCTGGCCAGCACC, to amplify a 497 bp product encoding up to UCR1, or GCGGCTGGGAGGGTCTTGGTCGCGGCGC, to amplify an 886 bp product encoding up to LR2 (Linker Region 2).

Molecular Pharmacology Fast Forward. Published on February 28, 2005 as DOI: 10.1124/mol.104.009423
This article has not been copyedited and formatted. The final version may differ from this version.

To assess the human tissue expression of PDE4A11 a panel of first strand cDNAs prepared from 24 human tissues (OriGene Technologies Inc., Rockville, MD) was used according to the manufacturers instructions. These were used as PCR templates to generate a 494 bp fragment using the sense primer GGAGCTGCAACTGGTGGC, designed to the unique N-terminal region of PDE4A11 and the anti-sense primer GGCACATTGGTCAGGAGTGAG, designed to the nucleotide sequence encoding LR1. The PCR was done using HotStar Taq DNA Polymerase (Qiagen) and PCR conditions 95^{o}C for 15 min and 35 cycles of 95^{o}C for 30 sec, 50^{o}C for 30 sec and 72^{o}C for 1 min. Final extension was carried out at 72^{o}C for 10 min and the PCR product was visualized as described above.

Transient expression of PDE4 isoforms in COS7 cells.

Transfection was done using the COS7 SV40-transformed monkey kidney cell line maintained at 37˚C in an atmosphere of 5% CO_2 / 95% air in complete growth medium containing DMEM supplemented with 0.1% penicillin/streptomycin (10000 units ml^{-1}), glutamine (2mM) and 10 % FCS. We have described this before in some detail (Huston et al., 1996; McPhee et al., 1999; Rena et al., 2001). Briefly, however, COS7 cells were transfected using DEAE Dextran. The DNA to be transfected (10μg) was mixed, and incubated for 15min with 200μl of 10mg ml^{-1} DEAE-dextran in PBS to give a 'DNA-dextran' mix. When cells reached 70% confluency, in 100mm dishes, the medium was removed and the cells were given 10ml of fresh DMEM containing 0.1mM chloroquine and the DNA-dextran mix (450μl). The cells were then incubated for 4h at 37˚C. After this period the medium was removed and the cells shocked with 10% DMSO in PBS. After PBS washing, the cells were returned to normal growth medium and left for a further two days before use. For determination of PDE activity the cells were homogenized in KHEM buffer (50mM KCl, 10mM EGTA, 1.92mM $MgCl_2$, 1mM dithiothreitol, 50mM Hepes, final pH7.2,) containing 'complete' protease inhibitors (Boehringer Mannheim) of final concentrations 40μg ml^{-1} PMSF, 156μg ml^{-1} benzamine, 1μg ml^{-1} aprotonin, 1μg ml^{-1} leupeptin, 1μg ml^{-1} pepstatin A and 1μg ml^{-1} antipain. As described previously (Huston et al., 1996; Rena et al., 2001; Sullivan et al., 1998), in such transfected cells then >98% of the total PDE activity was due to the recombinant

Molecular Pharmacology Fast Forward. Published on February 28, 2005 as DOI: 10.1124/mol.104.009423
This article has not been copyedited and formatted. The final version may differ from this version.

PDE4 isoform. In some instances the transfected COS7 cells were plated onto 6 well plates for use in experiments and then serum-starved over night before being treated with the indicated ligands for the stated lengths of time.

Luciferase reporter assays.

Human Embryonic Kidney (HEK) 293 cells were transfected using Transfast™ Transfection Reagent (Promega) and cotransfected with 1.2 μg firefly luciferase and 0.12 μg of the control Renilla luciferase construct pRL-CMV (Promega). The appropriate plasmids were then mixed with 45 μl serum free medium and 4 μl Transfast™ reagent. Following a 10 min incubation at room temperature, 40 μl DNA mix was added to the cells and incubated for 1hr at 37°C. They were then overlayed with 200 μl of DMEM. 48 hours after transfection the cells were lysed and assayed using the Dual Luciferaser Reporter Assay system (Promega) as described in the manufacturer's protocol using a Packard Fusion™ Universal Microplate Analyser. Luciferase activity values were normalised against the Renilla internal control.

Confocal analyses

PDE4A11 was transiently over-expressed and visualised in COS cells using PDE4A specific antisera as described previously by us for analyses of PDE4A4B (Huston et al., 1996; McPhee et al., 1999). Briefly, cells were transfected, using DOTAP (Roche), with the PDE4A11- pcDNA3 plasmid. Protein was expressed for 48h and cells were fixed in 4% paraformaldehyde containing 5% sucrose. After permeabilisation in 0.2% triton, proteins were blocked using 10% goat serum and 2% BSA before PDE4A11 was detected using an antibody raised against the C-terminus of human PDE4A and stained using alexa 594 (molecular probes). Cells were observed using a Zeiss Pascal laser scanning microscope.

For studies done on living cells GFP chimeras of PDE4A4B and PDE4A11 were used. COS cells were transfected with plasmids encoding in-frame fusions of either PDE4A4-GFP or PDE4A11-GFP using fugene6 (Roche). Proteins were expressed for 32h before rolipram (10μM) was added to the cells for a further 16h, essentially as previously described by us (Terry et al., 2003). PDE4A4-GFP and PDE4A11-GFP localisation was examined using a Zeiss Pascal laser scanning microscope.

Molecular Pharmacology Fast Forward. Published on February 28, 2005 as DOI: 10.1124/mol.104.009423
This article has not been copyedited and formatted. The final version may differ from this version.

Interaction with the SH3 domain of LYN and with βarrestin.

Assessment of the interaction of PDE4A11, PDE4A4 and PDE4A10 with the SH3 domain of LYN, expressed in E. Coli and subsequently purified to homogeneity, was done exactly as described in some detail previously by us for PDE4A10 (Rena et al., 2001) and other PDE4 species(Huston et al., 2000; McPhee et al., 1999). Briefly, volumes of slurry containing 400 ug of the fusion protein immobilized on glutathione agarose beads were pelleted and the supernatants discarded. Within each assay, volumes taken were equalized with washed beads. The pellets were resuspended in the cytosol from COS7 cells that had been transiently transfected to express the indicated PDE4A form. To allow for the binding of these various PDE4A long isoforms to LYN-SH3 to be compared an amount of cytosol fraction containing equal amounts of these enzymes, as assessed immunologically with PDE4A specific antisera, was taken. The amount of PDE4A4 was chosen such that about 80% became bound to LYN-SH3; this was usually of the order of 200 ug of lysate protein. These were diluted to a final volume of 200 ul in KHEM buffer containing 1 mM DTT and protease inhibitor cocktail. The immobilized fusion protein and cytosol were incubated together for 10 min end-over-end at 4°C. The beads were then collected by centrifugation and the supernatant retained as the unbound fraction. The beads were held on ice and washed three times with 400 ul of KHEM containing 1 mM DTT and protease inhibitor cocktail over a 15-min period. These washes were pooled along with the unbound fraction and aliquots taken for Western blotting along with the bead-bound PDE. This same method was employed to determine the putative interaction of the various PDE4A long isoforms with βarrestin, as described previously in some detail for PDE4D isoforms using a purified barrestin2-GST fusion protein generated in E coli with recombinant PDE4A isoforms expressed in COS7 cells (Bolger et al., 2003; Perry et al., 2002).

Action of Caspase-3 on PDE4A isoforms.

Recombinant caspase3 was generated in an active form as described before (Huston et al., 2000). 10ug of cytosolic COS-7 cell lysate expressing the indicated PDE4A isoforms was incubated for 2 h at 37 °C with recombinant caspase-3 as described previously by us (Huston et al., 2000). In order to normalize for the amount of mature

Molecular Pharmacology Fast Forward. Published on February 28, 2005 as DOI: 10.1124/mol.104.009423
This article has not been copyedited and formatted. The final version may differ from this version.

caspase-3, in each instance, an equal concentration (147 ng) of the p20 active caspase-3 subunit was added in a final volume of 25 ul of complete KHEM. Resultant protein was boiled in SDS sample buffer solution for Western blotting and probed with either an antibody raised to the common C-terminal region of PDE4A or an antibody specific to the N-terminal region of PDE4A4 (and PDE4A5) (Huston et al., 2000).

Assay of cAMP PDE activity

PDE activity was determined by a two-step procedure using 1μM cAMP as substrate, as described previously by us in some detail (see e.g. (Huston et al., 1996; Rena et al., 2001; Sullivan et al., 1998)). All assays were conducted at 30˚C with initial rates taken from linear time-courses. Activity was linear with added protein concentration.

Protein analysis.

Protein concentration was determined using BSA as standard.

Molecular Pharmacology Fast Forward. Published on February 28, 2005 as DOI: 10.1124/mol.104.009423
This article has not been copyedited and formatted. The final version may differ from this version.

Results.

The human PDE4A gene locus is located at chromosome 19p13.2 (Sullivan et al., 1998). Our sequencing and subsequent analysis (Sullivan et al., 1998) of a chromosome 19 cosmid contig containing the PDE4A gene locus led us to suggest that it may contain a hitherto unknown PDE4A long isoform. This was based on the finding of a sequence previously found in a cDNA clone, called TM3, which had been postulated to encode a catalytically inactive, C-terminally truncated protein (Bolger, 1994). However, the extreme 3' 360bp of the TM3 clone is not found in the human genome database. Indeed, it has been concluded (Sullivan et al., 1998) that this 'alien' sequence reflects the inverted 3' end of the pM5 cDNA. It is therefore likely that the TM3 clone is composed of two unrelated cDNAs that became inappropriately ligated during cloning. Thus the suggestion (Bolger et al., 1993) that TM3 reflects a truncated, catalytically inactive product of the PDE4A gene is, we believe, incorrect. The portion of the TM3 cDNA sequence found in the PDE4A containing contig is located between the single unique 5' exons that encode the PDE4A4B and PDE4A10 long isoforms (Fig. 1). As such it is appropriately positioned to provide a novel PDE4A long isoform. The prediction of this is that transcripts from any such novel long isoform, which we call here PDE4A11, should show sequence from the 5' exon spliced directly onto exon-2 of the PDE4A gene, rather than to more distant 3' exons characteristic of short and super-short isoforms.

Comparative genomics analysis of the human and murine PDE4A gene loci

The 38 kb region of the human PDE4A gene locus and the 33 kb region of the murine PDE4A gene locus were analysed by PROSCAN (http://bimas.dcrt.nih.gov/molbio/proscan/), a PolII promoter prediction program, the GRAIL CpG prediction program (http://compbio.ornl.gov/grailexp/) and the GENSCAN exon prediction program (http://genes.mit.edu/GENSCAN.html). Such comparative genomic analysis allowed us to identify a 5' exon for PDE4A11 (Fig 1a) that contained sequence found in the PDE4A11 (TM3) cDNA (Fig 1b). Also identified were sequences

Molecular Pharmacology Fast Forward. Published on February 28, 2005 as DOI: 10.1124/mol.104.009423
This article has not been copyedited and formatted. The final version may differ from this version.

immediately 5' to the exon-1^{4A11} that are conserved in human and mouse genes, which may be indicative of a functional promoter controlling PDE4A11 expression (see below).

The nucleotide sequence of exon-1^{4A11} was used to interrogate, using the BLAST algorithm, the expressed sequence tag (EST) database and high throughput sequence nucleotide databases. This allowed us to identify PDE4A11 sequences from various species, namely two mouse genomic draft sequences (GenBank AC027154 and AC073749), one rat genomic draft sequence (GenBank AC115140), seven human EST cDNAs (GenBank BI438716, BF732322, BF116176, AW296744, AW104482, CA775139 and CA774868), eight mouse EST cDNAs (GenBank BI56706, BY352528, BY184004, BY183996, BY353288, BY209230, BY352150 and BY347207), one bat EST cDNA (GenBank AC148813) and one pig EST cDNA (GenBank BX921915). All of these contained sequence showing high homology to that of the novel human PDE4A11-specific 5' sequence we identified here (Table 1). Importantly, however, it is clear (Table 1) that four of the human EST cDNAs (BI438716, AW104482, CA775139 and CA774868) also contained authentic sequence of human exons-2, -3, -4 and –5, three extended to exon-6, two to exon-7 and one to exon-8 within the catalytic unit (Table 1). These data clearly demonstrate splicing of the unique PDE4A11 5' exon-1 to the first long form exon, namely exon-2, indicating that PDE4A11 is indeed an authentic PDE4A long isoform. Consistent with this, inspection of the sequence of all the murine ESTs similarly shows splicing onto the murine exon-2 (Table 1). Additionally, the murine EST BI156706 showed a 98% match with the draft murine genomic sequence and analysis of the flanking genomic sequence revealed a consensus 5' splice acceptor site. Indeed, comparison of these human and murine PDE4A11 unique 5' sequences clearly revealed (Table 1) a conserved initiating methionine residue that predicts an in-frame ORF when spliced onto the common exon-2. Comparison (Fig 2) of the human and mouse unique PDE4A11 N-terminal regions reveals clear conservation between species, however this is clearly less than the 100% conservation seen for the human and murine unique N-terminal regions of PDE4A1 (Sullivan et al., 1998), PDE4A4 (Bolger et al., 1993; Huston et al., 1996; Sullivan et al., 1998) and PDE4A10 (Rena et al., 2001). Indeed, whilst the human PDE4A11 unique N-terminal region consists of 81 amino acids, that of murine PDE4A11 consists of only 66 amino acids (Fig. 2).

Molecular Pharmacology Fast Forward. Published on February 28, 2005 as DOI: 10.1124/mol.104.009423
This article has not been copyedited and formatted. The final version may differ from this version.

Expression Profile of PDE4A11

A schematic of the structure of PDE4 isoforms and the exons that encode it is shown in Fig 3a. The unique 5' exon of human PDE4A11 encodes the 81 amino acid unique N-terminal region of this isoform, whilst exons 2-15 encode the regulatory UCR1/2, the catalytic region and C-terminal portion (Fig. 3a). Using human brain RNA we were able to use RT-PCR to amplify from the unique 5' region of PDE4A11 into either the common UCR1 found only in full length PDE4 long isoforms and also into linker region 2 (LR2), which abuts the catalytic unit (Fig. 3b). We were also able to detect transcripts for PDE4A11 in RNA from HEK293 cells, using RT-PCR to amplify from the unique 5' region of PDE4A11 into the common UCR1 found only in full length PDE4 long isoforms (Fig 3b). This ability to undertake RT-PCR across the long form splice junction and into UCR1 confirms the EST data (Table 1) in identifying transcripts for PDE4A11 as a novel PDE4A long isoform.

We screened (Fig. 4a) a panel of RNA from various human tissues by RT-PCR using a sense primer targeted within the unique region of PDE4A11 and an anti-sense primer targeted within LR2 (Fig. 3a). This analysis identified transcripts for PDE4A11 in a variety of human tissues (Fig. 4a). The size of the transcript and its sequence (not shown) confirmed PDE4A11 as a long isoform as amplification was achieved across the conserved long form splice junction so as to encompass both UCR1 and UCR2 (Fig. 3a). Transcripts were most abundant in liver, stomach, testis, thyroid and adrenal glands but clearly evident in placenta, kidney, pancreas, ovary, uterus, and skin (Fig. 5a). Interestingly, whilst a clear signal for PDE4A11 transcripts was seen in foetal brain, little signal was seen in adult brain (Fig 4a). This might indicate a developmental change in PDE4A11 expression in brain and contrasts with PDE4A10, which is seemingly absent from foetal brain but seen clearly in adult brain (Rena et al., 2001). Indeed, PDE4A10 and PDE4A11 appear to show very distinct patterns of distribution (fig. 4a; (Rena et al., 2001)).

We also compared transcript levels for PDE4A11 relative to those for the PDE4A10 and PDE4A4B long isoforms in various human blood cell types (Fig. 4b). These data clearly show that PDE4A11 is widely expressed and, indeed, transcripts for it appear to provide the major species in a variety of cells including monocytes, mast cells

Molecular Pharmacology Fast Forward. Published on February 28, 2005 as DOI: 10.1124/mol.104.009423
This article has not been copyedited and formatted. The final version may differ from this version.

and macrophages as well as in bronchial smooth muscle. Conversely, PDE4A4B appears to provide the major level of transcripts in T cells (Fig. 4b).

Promoter activity of the 5' region of PDE4A11

The 1kb region immediately 5' of the ATG start in human exon-1^{4A11} was cloned into the vector pGL in order to evaluate any potential promoter activity by assessing the luciferase reporter function. This reporter construct was transfected into HEK293 cells whereupon a marked increase in luciferase activity was evident over that seen upon transfection of the base plasmid, pGL3 basic (Fig 5a). Alongside this, we compared the activity of the PDE4A10 promoter construct, which we have described previously (Rena et al., 2001), and the putative PDE4A4B promoter construct, which in all instance were similarly formed from 1kb of intronic sequence located immediately 5' to the ATG start site within exon-1^{4A10} and exon-1^{4A4B} , respectively (Fig. 5a). Interestingly, both the PDE4A11 and PDE4A10 promoter constructs gave similarly high activities in these cells, with less activity seen with the PDE4A4B construct (Fig. 5a). These data indicate that there is a functional promoter immediately upstream of the ATG start site in exon-1^{4A11}.

We then generated a panel of 5' deletion constructs of the PDE4A11 reporter construct and assessed their activity in HEK cells (Fig. 5b). Deletion of either 250bp or 500bp, to yield the '750bp' and '500bp' reporter constructs, led to little or no change in luciferase activity (Fig. 5b). Interestingly, deletion to yield the '250bp' construct led to a doubling of activity over that seen with the 500bb construct (Fig. 5b), implying that some repressor element may be functioning in the 250-500bp region. These data indicate that the first 250bp found immediately 5' to the ATG start site in exon-1^{4A11} contains elements that suffice to allow for promoter activity that we would expect to drive basal transcription of PDE4A11. Whilst this region does not contain a classical TATA box it is within a CpG-rich island (Fig 1b) and exhibits, as do a number of TATA-less promoters, a number of consensus sites for binding of the SP1 transcription factor, some of which are conserved between human and mouse (Fig. 5c).

Expression of recombinant PDE4A11 in COS7 cells

An expression construct of the entire ORF for PDE4A11, encoding 860 amino acids, was generated in pcDNA3. This was used for transient expression studies in

Molecular Pharmacology Fast Forward. Published on February 28, 2005 as DOI: 10.1124/mol.104.009423
This article has not been copyedited and formatted. The final version may differ from this version.

mammalian COS7 cells. COS7 cells transfected to express PDE4A11 exhibited a cAMP PDE activity of 4-6 nmol/min/mg protein, compared to the 4-6 pmol/min/mg protein seen in non-transfected cells (range: n=3). Assayed using 1μM cAMP as substrate, over 98% of the cAMP PDE activity in these cells was inhibited by the archetypal PDE4 selective inhibitor, rolipram (10μM). Thus recombinant PDE4A11 expressed in these cells shows the properties expected of a PDE4 family member and provides the major cAMP PDE activity in these transfected cells.

Immunoblotting (Fig 6a) of PDE4A11-transfected cells with a 'pan PDE4A' specific antiserum, generated against the C-terminal region found in common to all PDE4A isoforms identifies the presence of a single immunoreactive species of 126 +/- 4 kDa (mean +/- SD; n=3). The size of PDE4A11 on SDS-PAGE is comparable to that observed for the other two known PDE4A4 long isoforms, namely PDE4A4B (125 kDa) and PDE4A10 (121 kDa). Thus in endogenous expression systems these three long isoforms will not be readily distinguished by western blotting using pan 4A specific antisera. However, all are considerably larger than that of the 83 kDa PDE4A1 short isoform and all migrate on SDS-PAGE with substantially greater molecular weights than predicted by their primary amino acid sequence (Rena et al., 2001). Thus the predicted size of PDE4A11 is some 95.3kDa, which is around 30kDa less than that observed in SDS-PAGE. Deletion studies have shown that this aberrant migration is due to a region located within the conserved PDE4A catalytic core (Johnston et al., 2004).

Subcellular fractionation studies showed that some 52 ± 2 % (mean +/- SD; n=3) of PDE4A11 was located within the S2, high-speed supernatant fraction with the rest being particulate-associated. Immunohistochemical analysis, using confocal microscopy (Fig 6b) of COS7 cells transfected to express PDE4A11 showed that it was excluded from the nucleus and concentrated in the perinuclear region and at the cell margin.

We have demonstrated that chronic challenge of HEK, CHO and RBL cells expressing recombinant PDE4A4B caused a profound redistribution of PDE4A4B into foci within the cytoplasm (Terry et al., 2003). This reversible process is cAMP independent and presumed to be triggered as a consequence of a conformational change induced through the binding of the selective, competitive inhibitor rolipram to the active site of PDE4A4B. Such a profound redistribution was observed using wild-type PDE4A4

Molecular Pharmacology Fast Forward. Published on February 28, 2005 as DOI: 10.1124/mol.104.009423
This article has not been copyedited and formatted. The final version may differ from this version.

as well as chimeras formed with various tags including GFP, which allows for visualisation in living cells. Here we see, in living COS cells, that treatment with rolipram induced foci formation of GFP-tagged PDE4A4B (Fig. 6c). In marked contrast to this, however, rolipram treatment did not cause GFP-tagged versions of either PDE4A11 or PDE4A10 to form foci in these cells (Fig. 6c). As observed with untagged PDE4A11 (Fig 6b), GFP-tagged PDE4A11 in COS cells was concentrated in the perinuclear region and also observed within ruffles at the cell margin (Fig 6c). We noted that, unlike PDE4A11, neither PDE4A4 nor PDE4A10 were found within ruffles, highlighting this as a unique facet of the intracellular localisation of PDE4A11 (Fig. 6c).

Analysis of cAMP hydrolysis of soluble PDE4A11 showed it to have a K_m of 4.2 ± 1.1 uM and that of the particulate activity a K_m of 3.7 ± 1.8 uM (mean +/- SD; n=3). Such values are very similar to those exhibited by other PDE4 isoforms, including the PDE4A4B and PDE4A10 long isoforms (Huston et al., 1996; Rena et al., 2001). We then set out to evaluate how actively PDE4A11 hydrolysed cAMP compared to the other long PDE4A isoforms. To do this we took equal immunoreactive amounts of soluble PDE4A11 and PDE4A4B in order to determine a 'relative V_{max}' value. This yielded a ratio of 1.1 ± 0.1 (mean +/- SD; n=3) for the activity of PDE4A11 compared to PDE4A4B. From these data and that reported previously by us (Rena et al., 2001) the ratio of V_{max} values for long PDE4A isoforms was (1):1: 1.1 for PDE4A4B : PDE4A10 : PDE4A11, respectively. Thus all long PDE4A isoforms appear to be similarly active. We also noted that particulate association of PDE4A11 had little effect on its maximal catalytic activity, with the ratio of the V_{max} value for total particulate to soluble PDE4A11 being some 1.1 ± 0.1 (mean +/- SD; n=3).

Rolipram is the archetypal selective PDE4 inhibitor (Houslay and Adams, 2003). It dose-dependently inhibits cytosolic PDE4A11 activity with an IC_{50} value of 0.72 +/- 0.08 uM (mean +/- SD: n=3) (Fig. 7; Table 2). This is comparable to values of 0.056 μM and 1.25 μM for the soluble forms of PDE4A10 and PDE4A4B, respectively (Houslay, 2001; Huston et al., 1996; Rena et al., 2001).

PDE4A11 is also dose-dependently inhibited by a variety of other PDE4 selective inhibitors, namely Ro20-1724, cilomilast (Ariflo®), roflumilast and denbufylline (Fig. 8; Table 1). IC_{50} values range from around 1 uM for Ro20-1724 down

Molecular Pharmacology Fast Forward. Published on February 28, 2005 as DOI: 10.1124/mol.104.009423
This article has not been copyedited and formatted. The final version may differ from this version.

to around 4 nM with roflumilast® (Table 2). However, in each instance we noted that there was no difference in sensitivity of the cytosol and particulate forms of PDE4A11 to any particular inhibitor (Table 2). We also determined the sensitivity of PDE4A4 and PDE4A10 to inhibition by these various compounds (Table 2). In doing so we noted that PDE4A10 is considerably less sensitive to inhibition by Ariflo, whilst being considerably more sensitive to inhibition by rolipram, than either of the other two long isoforms (Table 2). Indeed, PDE4A11 appears to be slightly more sensitive to inhibition by Ariflo and denbufylline than either of the other two isoforms (Table 2). PDE4A4 appears to be slightly less sensitive to inhibition by Ro20-1724 than either of the other two long PDE4A isoforms (Table 2). We also see here that, as for rolipram, particulate PDE4A4 is more sensitive to inhibition by roflumilast, compared to its soluble form (Table 2).

The denaturation of enzyme proteins by heat occurs as a first order process that can be followed by analysis of the exponential decay in their catalytic activity. A semi-log plot of the log% activity remaining against time thus allows a determination of the half-life of inactivation ($T_{0.5}$). Here we see that incubation at 55˚C causes the inactivation of both soluble and particulate PDE4A11 as a single exponential (Fig. 8). However, in each of these instances there is a marked difference with half lives ($T_{0.5}$) of 2.5 ± 0.3 min for soluble PDE4A11 (S2 fraction) and 4.4 ± 0.3 min for particulate PDE4A11 (mean ± SD; n = 3 separate experiments).

Phosphorylation of PDE4A11 by PKA

Various long PDE4 isoforms can be activated through phosphorylation by PKA, which occurs at a consensus site (RRESF) for phosphorylation located in the PDE4 UCR1 regulatory module (Hoffmann et al., 1998; MacKenzie et al., 2002; Sette and Conti, 1996). Phosphorylation of this site by PKA can readily be monitored using an antiserum specific for the phosphorylated form of UCR1 (MacKenzie et al., 2002). Here we see that treatment of COS7 cells transfected to express PDE4A11 with the adenylyl cyclase activator, forskolin (100μM) together with the non-selective PDE inhibitor IBMX (100μM), in order to raise intracellular cAMP levels (MacKenzie et al., 2002) leads to the phosphorylation of PDE4A11 as indicated by the detection of a 126kDa immunoreactive species with the P-UCR1 antiserum (Fig. 9a). The appearance of this

Molecular Pharmacology Fast Forward. Published on February 28, 2005 as DOI: 10.1124/mol.104.009423
This article has not been copyedited and formatted. The final version may differ from this version.

126kDa immunoreactive species occurs in a time dependent fashion consequent upon the addition of forskolin and IBMX (Fig.9a) to COS7 cells and is not evident in non-transfected cells analysed under comparable levels of exposure in the ECL detection system (data not shown). The appearance of this immunoreactive species in cells challenged with forskolin together with IBMX is ablated in a dose dependent fashion when the PKA selective inhibitor, H89 is also present (Fig. 9b). When cells transfected to express the Ser119Ala-PDE4A11 construct, where the target serine for phosphorylation by PKA in UCR1 has been mutated to alanine, are challenged with forskolin together with IBMX then no immunoreactive species is detected with the P-UCR1 antiserum (Fig. 9c).

Treatment of COS7 cells expressing PDE4A11 with forskolin (100μM) together with IBMX (100μM) leads to the activation of PDE4A11 in a time-dependent fashion (Fig 9d), which reflects that seen for its phosphorylation (Fig. 9e). In contrast to this, challenge of COS7 cells expressing the Ser119Ala-PDE4A11 construct with forskolin (100μM) together with IBMX (100μM) did not lead to any change (<7%; n=3 experiments) in cAMP PDE activity. Similarly, no change in cAMP PDE activity (<6%) occurred in COS7 cells expressing PDE4A11 that were challenged with forskolin (100μM) together with IBMX (100μM) in the presence of the PKA inhibitor, H89.

Interaction of PDE4A11 with the SH3 domain of LYN.

Pull-down (sedimentation) assays have been used to show that the SH3 domain of LYN tyrosyl kinase, expressed as a GST fusion protein, binds to the long PDE4A4 isoform (McPhee et al., 1999; Rena et al., 2001). Deletion analyses then showed that the unique N terminus of PDE4A4 provided the major site of interaction, with the LR2 segment found in all active PDE4A isoforms providing another site of interaction (McPhee et al., 1999). Here we show that although PDE4A11 is able to interact with the SH3 domain of LYN, the magnitude of such interaction is less than that observed with PDE4A4 (Fig. 10a). Indeed, the degree of interaction is apparently similar to that seen using PDE4A10 (Fig. 10a).

Action of Caspase-3.

Molecular Pharmacology Fast Forward. Published on February 28, 2005 as DOI: 10.1124/mol.104.009423
This article has not been copyedited and formatted. The final version may differ from this version.

The rodent PDE4A5 isoform has been shown to provide a substrate for caspase-3 action (Huston et al., 2000). This cleaves at a single site within a caspase-3 consensus sequence (DAVD) located in the unique N-terminal region of PDE4A4. We see here that activated caspase-3 also acts on the 127kDa PDE4A4 isoform, which is the human homologue of PDE4A5, in order to yield a 120kDa species (Fig. 10b). This faster migrating, cleaved species is detected with the PDE4A C-terminal Ab. However, consistent with cleavage occurring in the unique N-terminal region of PDE4A4, such a faster migrating species is not seen using the PDE4A4 specific antiserum, which is targeted to the cleaved extreme N-terminal portion of PDE4A4 (Fig. 10b). However, it is apparent that the intensity of the signal detected by this PDE4A4 specific N-terminal antiserum is reduced in the caspase-3 treated track, consistent with a diminished amount of full length species due to caspase-3 action (Fig. 10b). The presumed site of cleavage in PDE4A4 by caspase-3 is the cognate one (D^{69}AMD) to that in PDE4D5 (D^{69}AVD), which would remove a circa 7ka fragment, consistent with the observed mobility shift (Fig. 10b). In contrast to this, caspase-3 failed to cause either any change in the mobility of PDE4A11 and PDE4A10 or any change in the intensity of the single immunoreactive species detected with the PDE4A C-terminal Ab (Fig 10). This is consistent with there not being any casapse-3 consensus motif within the unique N-terminal regions of either of these two species.

Interaction of PDE4A11 with βarrestin2

βarrestin seemingly has the potential to interact with PDE4 enzymes from all sub-families (Perry et al., 2002), which is presumed to result from a common binding site in the conserved PDE4 catalytic unit (Bolger et al., 2003). Given that the catalytic unit of PDE4 isoforms within a subfamily may be affected by the N-terminal region, as indicated by different thermostability and inhibitor sensitivities, we set out here to determine whether these three PDE4 isoforms could potentially interact with βarrestin. As done before by us for PDE4D, we used a pull-down assay with βarrestin-GST and the various PDE4A isoforms expressed in E coli. Using equal immunoreactive mounts of each of these three isoforms we see here that all three species can interact with βarrestin (Fig. 10c).

Molecular Pharmacology Fast Forward. Published on February 28, 2005 as DOI: 10.1124/mol.104.009423
This article has not been copyedited and formatted. The final version may differ from this version.

Discussion

PDE4 isoforms provide targets for novel anti-inflammatory therapeutics (Burnouf and Pruniaux, 2002; Giembycz, 2002) and serve to determine compartmentalised cAMP signalling (Mongillo et al., 2004). Here we have identified a novel human PDE4A long isoform, called PDE4A11, which is highly conserved amongst species (Fig. 2). Available sequence for the unique portion of PDE4A11 (Fig. 2a) indicates that whilst pig and bat sequences show 90% identity with human PDE4A11, this falls to 54% in rodents, suggesting caution in extrapolating data from rodent studies to human.

Transcript analysis (Fig. 4) indicates that PDE4A11 is widely expressed in human tissues including cells involved in inflammatory responses. Indeed, PDE4A11 transcript levels are invariably similar to, or even greater than, those of the two other known PDE4A long isoforms, PDE4A4B (Bolger et al., 1993) and PDE4A10 (Rena et al., 2001). Whilst, to date, attention has focussed on PDE4A4B, levels of PDE4A4B transcripts appear to be in lowest abundance (Fig. 4). Ideally we would have liked to undertake immunological analyses. However, we have been unsuccessful in trying to generate PDE4A11 specific antisera.

We have identified a functional promoter for PDE4A11, with basal activity contained within a 250bp region located immediately 3' to the ATG start site for PDE4A11 (Fig 5). As with all PDE4 isoform promoters identified to date (Le Jeune et al., 2002; Rena et al., 2001; Vicini and Conti, 1997), this region contains a series of perfect stimulating protein 1 (Sp1) consensus binding sites. Such sites typically drive basal transcription of genes that like those for PDE4 isoforms lack a canonical TATA box and reside in CpG-rich islands. In this 250bp region there are potential binding sites for early growth response-1 (Egr-1), GATA-1/2/3 and AML-1a transcription factors, which have been shown to synergise with Sp1 in driving basal promoter activity of various genes (see e.g. (Alfonso-Jaume et al., 2004)). Two of the putative Sp1 sites have overlapping CACCC binding factor sites, a situation that in the monoamine oxidase_B gene confers inhibitory regulation (Ou et al., 2004).

Molecular Pharmacology Fast Forward. Published on February 28, 2005 as DOI: 10.1124/mol.104.009423
This article has not been copyedited and formatted. The final version may differ from this version.

PDE4A long isoforms differ from each other by their unique N-terminal regions, which are encoded by distinct 5' exons (Houslay and Adams, 2003; Sullivan et al., 1998). In the case of PDE4A11, exon1^{4A11} encodes a region of 81 amino acids that bears no similarity to that of any other known PDE4 isoform. The core PDE4A species is an entirely cytosolic entity (Sullivan et al., 1998), indicating that the N-terminal region of PDE4A11, like that of other PDE4 isoforms (Baillie et al., 2002; Huston et al., 1996; McPhee et al., 1999; Rena et al., 2001), has a role in intracellular targeting. Here we see that PDE4A11 is primarily localised to the perinuclear region but is also found in ruffles at the cell plasma membrane, as shown for the wild-type PDE4A11 in fixed cells and for GFP-chimera in living cells (Fig 6). Cell disruption identifies a soluble component, although it is unclear as to whether this reflects cytosolic PDE4A11 or PDE4A11 that reversibly and weakly binds to particulate anchor proteins and is released upon cell breakage.

As reported previously (Terry et al., 2003), chronic treatment of COS cells with rolipram causes a profound change on the intracellular distribution of PDE4A4B, namely its reversible relocalisation to foci within cells (Fig. 6c). Such a re-organisation is induced by a conformational change in PDE4A4B occurring upon rolipram binding (Terry et al., 2003). This is specific to PDE4A4, rather than generic for PDE4A long isoforms, as neither PDE4A11 nor PDE4A10 show any such redistribution. Indeed, PDE4A4B (McPhee et al., 1999), but neither PDE4A11 nor PDE4A10 (Table 2), exhibit a dramatic increase in affinity for rolipram upon membrane binding. This identifies PDE4A4B alone as being peculiarly sensitive to conformational changes involving rolipram.

Thermal denaturation analyses provide a simple means of evaluating differences in the conformational status of closely related proteins. We have shown (Rena et al., 2001) that whilst incubation at 55°C causes the inactivation of PDE4A4B and PDE4A10 to occur as single exponentials, this is characterised by very different half lives. Thus cytosolic PDE4A4B is more thermostable ($T_{0.5}$ = 22min) than PDE4A10 ($T_{0.5}$ = 11 min). Here we see that PDE4A11 is different again, with the cytosolic enzyme being dramatically more labile, decaying with a half life ($T_{0.5}$) of 2.5min (Fig. 8). The unique N-terminal region of each of these isoforms appears to exert a distinct effect on the

Molecular Pharmacology Fast Forward. Published on February 28, 2005 as DOI: 10.1124/mol.104.009423
This article has not been copyedited and formatted. The final version may differ from this version.

conformational status of the PDE4A catalytic unit. The functional significance of this remains to be ascertained although, clearly, it does not translate into any change in catalytic activity as the K_m values and relative V_{max} values of these isoforms are near identical. Interestingly, however, whilst particulate PDE4A11 is more thermostable ($T_{0.5}$ = 4.4 min) than its cytosolic component (Fig. 8), the converse is true for both PDE4A10 ($T_{0.5}$ = 5 min) and PDE4A4B ($T_{0.5}$ = 12.5min) (Rena et al., 2001). As the N-terminal regions of PDE4 isoforms have an important role in intracellular targeting (Conti et al., 2003; Houslay and Adams, 2003) our data suggests that particulate association exerts distinct effects on the conformational status of each of these isoforms. Indeed, the N-terminal domain together with LR2 allow PDE4A4 to interact with the SH3 domains of SRC family tyrosyl kinases, particularly LYN (McPhee et al., 1999). The N-terminal interaction affects intracellular targeting (Beard et al., 2002), whilst the combined interaction at these two sites affects the conformation of the catalytic unit of PDE4A4 (McPhee et al., 1999). PDE4A11 and PDE4A10 lack consensus sites for SH3 domain interaction in their unique N-terminal regions, thus interaction is confined to the common LR2 region, explaining their reduced interaction, compared to PDE4A4, with the SH3 domain of LYN (Fig. 10a). Differences in interaction with proteins may contribute to altered conformations of these isoforms, with changed functional attributes and altered thermostability. In this regard, βarrestins, which act as a multifunctional scaffold protein responsible for desensitizing G-protein coupled receptors (Perry and Lefkowitz, 2002), have recently been show to bind PDE4 enzymes, thereby recruiting active PDEs to the site of cAMP synthesis in cells (Perry et al., 2002). We show here that all three PDE4A long isoforms have the potential to interact with βarrestin2 (Fig. 10c). This is consistent with the notion that βarrestins bind to a common binding site in the conserved PDE4 catalytic unit (Bolger et al., 2003). It also indicates that whatever differences there may be in the conformation of the catalytic unit of these PDE4A isoforms, as gauged from altered thermostability and inhibitor sensitivity, this does not extend to ablating interaction with βarrestin2.

PDE4A11 is inhibited by a number of PDE4 selective inhibitors, including cilomilast (Ariflo®) and roflumilast (Table 2), which are currently undergoing clinical

Molecular Pharmacology Fast Forward. Published on February 28, 2005 as DOI: 10.1124/mol.104.009423
This article has not been copyedited and formatted. The final version may differ from this version.

trials (Gamble et al., 2003; Spina, 2003; Timmer et al., 2002). In this we note that roflumilast is by far the most potent of these inhibitors, with an IC_{50} value some 150-fold lower than that of the archetypal PDE4 inhibitor, rolipram (Table 2). We also show that there is no difference in the sensitivity of the particulate, compared to the soluble, forms of PDE4A11 to inhibition by these compounds (Table 2). As seen with activity analyses, the conformational difference in particulate versus soluble PDE4A11 detected by thermostability studies does not extend to any effect on inhibitor action. PDE4A4B thus remains the only identified PDE4A isoform where rolipram more potently inhibits the particulate enzyme compared to the cytosolic species (Huston et al., 1996; McPhee et al., 1999). We did observe some subtle differences in inhibition of these three PDE4A long isoforms. Thus PDE4A11 is somewhat more sensitive to inhibition by Ariflo and denbufylline than either PDE4A4 or PDE4A10 (Table 2). Indeed, PDE4A11 and PDE4A10 are somewhat more sensitive to inhibition by Ro20-1724 than PDE4A4 (Table 2). Furthermore, PDE4A10 is considerably less sensitive to inhibition by Ariflo, whilst being considerably more sensitive to inhibition by rolipram, than either PDE4A4 or PDE4A11 (Table 2).

The UCR1 regulatory module of all PDE4 isoforms contains a consensus site (RRESF) for phosphorylation by PKA. Studies done on PDE4D3, and later other isoforms, showed that PKA phosphorylates the serine in this motif, causing enzyme activation (Hoffmann et al., 1998; MacKenzie et al., 2002; Sette and Conti, 1996). This has physiological significance in providing part of the cellular desensitization system to cAMP action (Oki et al., 2000). We have shown (MacKenzie et al., 2002; Rena et al., 2001) that PKA can phosphorylate PDE4 long isoforms from a variety of subfamilies, although activation is typically around 50%, compared to the 2-3 fold seen uniquely with PDE4D3 where such amplification is presumed to be determined by the unique N-terminal region of PDE4D3. Here we show that, in intact cells challenged with forskolin and IBMX so as to elevate intracellular cAMP levels, PDE4A11 is phosphorylated at Ser119 in UCR1, whereupon it is activated by around 80% (Fig. 9). This shows that PDE4A11 can also be regulated by PKA-mediated phosphorylation.

In order to begin to understand the role of PDE4 enzymes in cell biology and as therapeutic targets it is crucial to appreciate the full range of isoforms. Here we have

Molecular Pharmacology Fast Forward. Published on February 28, 2005 as DOI: 10.1124/mol.104.009423
This article has not been copyedited and formatted. The final version may differ from this version.

identified a novel, widely expressed PDE4A long isoform whose unique N-terminal region determines intracellular targeting and exerts a conformational action on this isoform that is clearly evident from the various differences noted here when compared to other PDE4A long isoforms (Table 3). When cAMP levels are elevated in cells PDE4A11 becomes phosphorylated and activated by PKA. This feature, together with its intracellular targeting, shows that PDE4A11 is poised to contribute to compartmentalised cAMP signalling and desensitization. Indeed, of all three known PDE4A long isoforms it is transcripts for PDE4A11 that we show here to be the highest by far, compared to either PDE4A10 or PDE4A4, in cells associated with inflammatory responses, such as monocytes, macrophages, eosinophils. This might suggest that PDE4A11 could provide a novel target in the future for therapeutics aimed at particular isoforms, such as those using siRNA.

Molecular Pharmacology Fast Forward. Published on February 28, 2005 as DOI: 10.1124/mol.104.009423
This article has not been copyedited and formatted. The final version may differ from this version.

Acknowledgements

We would like to thank Jennifer M. Wilson and Frank P. Maurio (GSK) for their help with Taqman analyses. The sequence for PDE4A11 has been deposited in GenBank (AY618547).

Molecular Pharmacology Fast Forward. Published on February 28, 2005 as DOI: 10.1124/mol.104.009423
This article has not been copyedited and formatted. The final version may differ from this version.

References

Alfonso-Jaume MA, Mahimkar R and Lovett DH (2004) Co-operative interactions between NFAT (nuclear factor of activated T cells) c1 and the zinc finger transcription factors Sp1/Sp3 and Egr-1 regulate MT1-MMP (membrane type 1 matrix metalloproteinase) transcription by glomerular mesangial cells. *Biochem J* **380**:735-47.

Baillie GS, Huston E, Scotland G, Hodgkin M, Gall I, Peden AH, MacKenzie C, Houslay ES, Currie R, Pettitt TR, Walmsley AR, Wakelam MJ, Warwicker J and Houslay MD (2002) TAPAS-1, a Novel Microdomain within the Unique N-terminal Region of the PDE4A1 cAMP-specific Phosphodiesterase That Allows Rapid, Ca2+- triggered Membrane Association with Selectivity for Interaction with Phosphatidic Acid. *J Biol Chem* **277**:28298-28309.

Baillie GS, MacKenzie SJ, McPhee I and Houslay MD (2000) Sub-family selective actions in the ability of Erk2 MAP kinase to phosphorylate and regulate the activity of PDE4 cyclic AMP-specific phosphodiesterases. *Br J Pharmacol* **131**:811-819.

Baillie GS, Sood A, McPhee I, Gall I, Perry SJ, Lefkowitz RJ and Houslay MD (2003) beta-Arrestin-mediated PDE4 cAMP phosphodiesterase recruitment regulates beta-adrenoceptor switching from Gs to Gi. *Proc Natl Acad Sci U S A* **100**:940-5.

Barber R, Baillie GS, Bergmann R, Shepherd MC, Sepper R, Houslay MD and Heeke GV (2004) Differential expression of PDE4 cAMP phosphodiesterase isoforms in inflammatory cells of smokers with COPD, smokers without COPD, and nonsmokers. *Am J Physiol Lung Cell Mol Physiol* **287**:L332-43.

Beard MB, Huston E, Campbell L, Gall I, McPhee I, Yarwood S, Scotland G and Houslay MD (2002) In addition to the SH3 binding region, multiple regions within the N- terminal noncatalytic portion of the cAMP-specific phosphodiesterase, PDE4A5, contribute to its intracellular targeting. *Cell Signal* **14**:453-65.

Beavo JA and Brunton LL (2002) Cyclic nucleotide research -- still expanding after half a century. *Nat Rev Mol Cell Biol* **3**:710-8.

Bolger G, Michaeli T, Martins T, St John T, Steiner B, Rodgers L, Riggs M, Wigler M and Ferguson K (1993) A family of human phosphodiesterases homologous to the dunce learning and memory gene product of Drosophila melanogaster are potential targets for antidepressant drugs. *Mol Cell Biol* **13**:6558-71.

Bolger GB (1994) Molecular biology of the cyclic AMP-specific cyclic nucleotide phosphodiesterases: a diverse family of regulatory enzymes. *Cell Signal* **6**:851-9.

Bolger GB, McCahill A, Huston E, Cheung YF, McSorley T, Baillie GS and Houslay MD (2003) The unique amino-terminal region of the PDE4D5 cAMP phosphodiesterase isoform confers preferential interaction with beta-arrestins. *J Biol Chem* **278**:49230-8.

Burnouf C and Pruniaux MP (2002) Recent advances in PDE4 inhibitors as immunoregulators and anti-inflammatory drugs. *Curr Pharm Des* **8**:1255-96.

Molecular Pharmacology Fast Forward. Published on February 28, 2005 as DOI: 10.1124/mol.104.009423
This article has not been copyedited and formatted. The final version may differ from this version.

Chapman CG, Meadows HJ, Godden RJ, Campbell DA, Duckworth M, Kelsell RE, Murdock PR, Randall AD, Rennie GI and Gloger IS (2000) Cloning, localisation and functional expression of a novel human, cerebellum specific, two pore domain potassium channel. *Brain Res Mol Brain Res* **82**:74-83.

Conti M, Richter W, Mehats C, Livera G, Park JY and Jin C (2003) Cyclic AMP-specific PDE4 Phosphodiesterases as Critical Components of Cyclic AMP Signaling. *J Biol Chem* **278**:5493-6.

Gamble E, Grootendorst DC, Brightling CE, Troy S, Qiu Y, Zhu J, Parker D, Matin D, Majumdar S, Vignola AM, Kroegel C, Morell F, Hansel TT, Rennard SI, Compton C, Amit O, Tat T, Edelson J, Pavord ID, Rabe KF, Barnes NC and Jeffery PK (2003) Antiinflammatory effects of the phosphodiesterase-4 inhibitor cilomilast (Ariflo) in chronic obstructive pulmonary disease. *Am J Respir Crit Care Med* **168**:976-82.

Giembycz MA (2002) Development status of second generation PDE4 inhibitors for asthma and COPD: the story so far. *Monaldi Arch Chest Dis* **57**:48-64.

Hoffmann R, Wilkinson IR, McCallum JF, Engels P and Houslay MD (1998) cAMP-specific phosphodiesterase HSPDE4D3 mutants which mimic activation and changes in rolipram inhibition triggered by protein kinase A phosphorylation of Ser-54: Generation of a molecular model. *Biochemical Journal* **333**:139-149.

Houslay MD (2001) PDE4 cAMP-specific phosphodiesterases. *Prog Nucleic Acid Res Mol Biol* **69**:249-315.

Houslay MD and Adams DR (2003) PDE4 cAMP phosphodiesterases: modular enzymes that orchestrate signalling cross-talk, desensitization and compartmentalization. *Biochem J* **370**:1-18.

Huston E, Beard M, McCallum F, Pyne NJ, Vandenabeele P, Scotland G and Houslay MD (2000) The cAMP-specific phosphodiesterase PDE4A5 is cleaved downstream of its SH3 interaction domain by caspase-3. Consequences for altered intracellular distribution. *J Biol Chem* **275**:28063-74.

Huston E, Pooley L, Julien P, Scotland G, McPhee I, Sullivan M, Bolger G and Houslay MD (1996) The human cyclic AMP-specific phosphodiesterase PDE-46 (HSPDE4A4B) expressed in transfected COS7 cells occurs as both particulate and cytosolic species that exhibit distinct kinetics of inhibition by the antidepressant rolipram. *J Biol Chem* **271**:31334-44.

Johnston LA, Erdogan S, Cheung YF, Sullivan M, Barber R, Lynch MJ, Baillie GS, Van Heeke G, Adams DR, Huston E and Houslay MD (2004) Expression, intracellular distribution and basis for lack of catalytic activity of the PDE4A7 isoform encoded by the human PDE4A cAMP-specific phosphodiesterase gene. *Biochem J* **380**:371-84.

Le Jeune IR, Shepherd M, Van Heeke G, Houslay MD and Hall IP (2002) Cyclic AMP-dependent Transcriptional Up-regulation of Phosphodiesterase 4D5 in Human Airway Smooth Muscle Cells: IDENTIFICATION AND CHARACTERIZATION OF A NOVEL PDE4D5 PROMOTER. *J Biol Chem* **277**:35980-35989.

MacKenzie SJ, Baillie GS, McPhee I, Bolger GB and Houslay MD (2000) ERK2 MAP kinase binding, phosphorylation and regulation of PDE4D cAMP specific

phosphodiesterases: the involvement of C-terminal docking sites and N-terminal UCR regions. *J. Biol. Chem.* **275**:16609-16617.

MacKenzie SJ, Baillie GS, McPhee I, MacKenzie C, Seamons R, McSorley T, Millen J, Beard MB, van Heeke G and Houslay MD (2002) Long PDE4 cAMP specific phosphodiesterases are activated by protein kinase A-mediated phosphorylation of a single serine residue in Upstream Conserved Region 1 (UCR1). *Br J Pharmacol* **136**:421-33.

Maurice DH, Palmer D, Tilley DG, Dunkerley HA, Netherton SJ, Raymond DR, Elbatarny HS and Jimmo SL (2003) Cyclic nucleotide phosphodiesterase activity, expression, and targeting in cells of the cardiovascular system. *Mol Pharmacol* **64**:533-46.

McPhee I, Yarwood SJ, Huston E, Scotland G, Beard MB, Ross AH, Houslay ES and Houslay MD (1999) Association with the src family tyrosyl kinase lyn triggers a conformational change in the catalytic region of human cAMP-specific phosphodiesterase HSPDE4A4B: consequences for rolipram inhibition. *J. Biol. Chem.* **274**:11796-11810.

Mehats C, Jin SL, Wahlstrom J, Law E, Umetsu DT and Conti M (2003) PDE4D plays a critical role in the control of airway smooth muscle contraction. *Faseb J* **17**:1831-41.

Mongillo M, McSorley T, Evellin S, Sood A, Lissandron V, Terrin A, Huston E, Hannawacker A, Lohse MJ, Pozzan T, Houslay MD and Zaccolo M (2004) Fluorescence resonance energy transfer-based analysis of cAMP dynamics in live neonatal rat cardiac myocytes reveals distinct functions of compartmentalized phosphodiesterases. *Circ Res* **95**:67-75.

Oki N, Takahashi SI, Hidaka H and Conti M (2000) Short term feedback regulation of cAMP in FRTL-5 thyroid cells. Role Of pde4d3 phosphodiesterase activation. *J Biol Chem* **275**:10831-7.

Ou XM, Chen K and Shih JC (2004) Dual functions of transcription factors, transforming growth factor-beta-inducible early gene (TIEG)2 and Sp3, are mediated by CACCC element and Sp1 sites of human monoamine oxidase (MAO) B gene. *J Biol Chem* **279**:21021-8.

Perry SJ, Baillie GS, Kohout TA, McPhee I, M.M. M, Ang KL, Miller WE, McLean AJ, Conti M, Houslay MD and Lefkowitz RJ (2002) Targeting of cyclic AMP degradation to β2-adrenergic receptors by β-arrestins. *Science* **298**:834-836.

Perry SJ and Lefkowitz RJ (2002) Arresting developments in heptahelical receptor signaling and regulation. *Trends Cell Biol* **12**:130-8.

Rena G, Begg F, Ross A, MacKenzie C, McPhee I, Campbell L, Huston E, Sullivan M and Houslay MD (2001) Molecular cloning and characterization of the novel cAMP specific phosphodiesterase, PDE4A10. *Mol. Pharmacol.* **59**:996-1011.

Sette C and Conti M (1996) Phosphorylation and activation of a cAMP-specific phosphodiesterase by the cAMP-dependent protein kinase. Involvement of serine 54 in the enzyme activation. *Journal of Biological Chemistry* **271**:16526-16534.

Shepherd MC, Baillie GS, Stirling DI and Houslay MD (2004) Remodelling of the PDE4 cAMP phosphodiesterase isoform profile upon monocyte-macrophage differentiation of human U937 cells. *Br J Pharmacol* **142**:339-51.

Molecular Pharmacology Fast Forward. Published on February 28, 2005 as DOI: 10.1124/mol.104.009423
This article has not been copyedited and formatted. The final version may differ from this version.

Spina D (2003) Phosphodiesterase-4 inhibitors in the treatment of inflammatory lung disease. *Drugs* **63**:2575-94.

Sullivan M, Rena G, Begg F, Gordon L, Olsen AS and Houslay MD (1998) Identification and characterization of the human homologue of the short PDE4A cAMP-specific phosphodiesterase RD1 (PDE4A1) by analysis of the human HSPDE4A gene locus located at chromosome 19p13.2. *Biochem J* **333**:693-703.

Terry R, Cheung YF, Praestegaard M, Baillie GS, Huston E, Gall I, Adams DR and Houslay MD (2003) Occupancy of the catalytic site of the PDE4A4 cyclic AMP phosphodiesterase by rolipram triggers the dynamic redistribution of this specific isoform in living cells through a cyclic AMP independent process. *Cell Signal* **15**:955-71.

Timmer W, Leclerc V, Birraux G, Neuhauser M, Hatzelmann A, Bethke T and Wurst W (2002) The new phosphodiesterase 4 inhibitor roflumilast is efficacious in exercise-induced asthma and leads to suppression of LPS-stimulated TNF-alpha ex vivo. *J Clin Pharmacol* **42**:297-303.

Vicini E and Conti M (1997) Characterization of an intronic promoter of a cyclic adenosine 3',5'- monophosphate (cAMP) - Specific phosphodiesterase gene that confers hormone and cAMP inducibility. *Molecular Endocrinology* **11**:839-850.

Footnotes

†Financial support:- DW thanks the BBSRC and GSK for a CASE research studentship. MDH thanks the Medical Research Council UK (G8604010) and the European Union (QLG2-CT-2001-02278; QLK3-CT-2002-02149) for grant support.

¶ to whom all correspondence should be addressed.
Email M.Houslay@bio.gla.ac.uk, phone +44-(0)141-330-5803, fax +44-(0)141-330-4365

[4] present address:- Randox Laboratories Ltd., 55 Diamond Road, Crumlin, County Antrim, BT29 4QY, Northern Ireland

[5] present address:- CSC, DuPont Teijin Films, Dalbeattie Rd., Dumfries, DG2 8YA

[6] present address:- GlaxoSmithKline, Corporate Intellectual Property, New Frontiers Science Park, Third Avenue, Harlow, Essex CM19 5AW, UK

[7] present address:- EvoQuest Custom Services, InVitrogen, 3 Fountain Drive, Inchinnan Business Park, PA4 9RF, UK

Molecular Pharmacology Fast Forward. Published on February 28, 2005 as DOI: 10.1124/mol.104.009423
This article has not been copyedited and formatted. The final version may differ from this version.

Figure Legends

Figure 1. Schematic representation of the disposition of unique 5' exons in the PDE4A gene

(a) Shows the organisation of the unique 5' exons (exon-1) that encode the N-terminal regions of the PDE4A4B, PDE4A10 and novel PDE4A11 isoforms in the *PDE4A* gene as well as the first common exon (exon-2) used by all these three long isoforms. (b) Human genomic sequence showing exon 1 of the PDE4A11 splice variant. Nucleotides in bold show the coding region of Exon1^{4A11}. The nucleotide sequence underlined is the region identified as a CpG rich island.

Figure 2. Alignments of the predicted amino acid sequence encoded by the PDE4A11 unique 5' exon from various species.

(a) Alignments are shown for the amino acid sequence encoded by cognate PDE4A11 5' exons found in genomic sequences from man (GenBank AC011548), bat (GenBank AC148813), mouse (GenBank AC027154 and AC073749) and rat (GenBank AC148813). In (b) the sequences for the authentic 3' splice sites for mouse, rat and bat are shown.

Figure 3. PDE4A11 is a long isoform encoded by the PDE4A gene.

(a) in the upper panel shows a schematic of the key regions of PDE4A11 as inferred from EST analysis and by reference to the structure of established PDE4 long isoforms. Shown schematically are the N-terminal regions unique to the three long PDE4A isoforms, namely PDE4A4B (GenBank L20965), PDE4A10 (GenBank AF110461) and PDE4A11 (GenBank AY618547). Also indicated are the positions of primers used in RT-PCR studies, for which sequence details are given in the Methods.

Molecular Pharmacology Fast Forward. Published on February 28, 2005 as DOI: 10.1124/mol.104.009423
This article has not been copyedited and formatted. The final version may differ from this version.

UCR – Upstream Conserved Region; LR – Linker Region and CLFR- common long form region as described in (Houslay, 2001). Assuming ATG = 123 in the 4A11 ORF, then 4A11 NT Sense RT-PCR probe is nucleotides 1-25; 4A11 UCR1 Anti-sense RT-PCR probe is nucleotides 471-497; 4A11 LR2 Anti-sense RT-PCR probe is nucleotides 859-886; 4A11 Expression profile Sense probe is nucleotides 33-50 and 4A11 Expression profile Anti-sense probe is nucleotides 507-527. Prove sequences are given in Methods. In the lower panel the coding exons (boxes) for active PDE4A isoforms, with the unique 5' exons shown as filled boxes, are shown schematically. PDe4A1 is a super-short isoform that lacks UCR1 and has a truncated UCR2, whilst PDE4A4B, PDE4A10 and PDE4A11 are long isoforms.

(b) in the left panel is an RT-PCR analysis done on human brain mRNA with a sense primer targeted within the unique region of PDE4A11 and an anti-sense primer targeted within either UCR1 or LR2, as indicated. In the right hand panel is an RT-PCR analysis done on HEK293 cells with a sense primer targeted within the unique region of PDE4A11 and an anti-sense primer targeted within UCR1.

Figure 4 Expression profile of PDE4A11.

(a) RT-PCR analysis of the distribution of transcripts for PDE4A11 as identified in a panel of human RNA probed by RT-PCR using a sense primer targeted within the unique region of PDE4A11 and an anti-sense primer targeted within LR1. The data shown are representative of an experiment done three times.

(b) TaqMan mRNA profiles assessing the distribution of transcripts for PDE4A4B, PDE4A10 and PDE4A11 in various human blood cell types as well as bronchial epithelium and bronchial smooth muscle. These data are from cells pooled from 3 normal individuals.

Figure 5 Promoter activity associated with the intron upstream of the unique PDE4A11 5' exon.

(a) Shows the results of luciferase reporter assays for three putative promoter evaluation constructs. These were formed by cloning 1kb regions located immediately 5'

Molecular Pharmacology Fast Forward. Published on February 28, 2005 as DOI: 10.1124/mol.104.009423
This article has not been copyedited and formatted. The final version may differ from this version.

of each of the human exon-1^{4A4b} , exon-1^{4A10} and exon-1^{4A11} into the vector pGL. These were then transfected into HEK293 cells in order to evaluate any potential promoter activity of these constructs by assessing luciferase activity. Data are shown as relative (%) to that observed with the PDE4A11 construct (100%) for n=5 separate transfections (means ± SD).

(b) Shows luciferase reporter assay for various 5' truncates of the 1kb putative PDE4A11 promoter construct (as above) transfected into HEK293 cells with data are shown as relative (%) to the maximal activity observed (100%), in this case with the construct formed from 250bp immediately upstream of the unique PDE4A11 exon (data are means ± SD for n=4 separate transfections).

(c) Comparison of the 250bp of intronic sequence found immediately upstream of the ATG start site for PDE4A11 in both human and mouse. Examples of putative transcription binding sites are indicated. Sp1** are completely conserved in human and mouse, Sp1* are highly conserved in human and mouse whilst Sp1 are unique to human. Filled in blocks represent conserved sequence.

Figure 6. Expression of recombinant PDE4A11 in COS7 cells.

(a) Shown is a western blot of lysates from COS7 cells that either had (Tr) or had not (Ctr) been transfected with a plasmid encoding PDE4A11. In the transfected cells a single 126kDa immunoreactive species was identified using a 'pan PDE4A' antiserum able to detect all active human PDE4A isoforms.

(b) Shown is a confocal section through a fixed COS7 cell transfected to express wild-type PDE4A11 and visualised immunologically using a human PDE4A specific antiserum. Note that fluorescence is focused towards the perinuclear region of the cell with also centres of fluorescence located at the cell margin, as indicated by the white arrows. At similar gain then no fluorescence was evident in cells that had either not been transfected or transfected with empty vector.

(c) Shown are confocal sections through living COS cells transfected to express C-terminal GFP-tagged forms of PDE4A4B, PDE4A11 and PDE4A10, as indicated. Additionally shown are such cells that had been incubated for 16h with rolipram (10μM).

Molecular Pharmacology Fast Forward. Published on February 28, 2005 as DOI: 10.1124/mol.104.009423
This article has not been copyedited and formatted. The final version may differ from this version.

In the panel showing rolipram-treated cells expressing PDE4A4B, then the white arrows indicate examples of foci. In the panels showing untreated cells expressing PDE4A11 then the white arrows indicate examples of PDE4A11 located within ruffles at the cell margins.

These data are typical of experiments done at least three times with different transfections.

Figure 7. Inhibition of PDE4A11 by selective PDE4 inhibitors.

cAMP PDE activity assays on PDE4A11 were performed using 1μM cAMP as substrate with the range of inhibitor concentrations and type of inhibitor as indicated in each graph. The structures of the various inhibitors used in this study are provided in a file deposited as on-line supplementary information associated with this article on the Molecular Pharmacology website. Analyses were done both on soluble (S2) fraction PDE4A11 as well as particulate (P1 + P2) associated PDE4A11 The data are averages for three separate experiment shown as means ± SD.

Figure 8. Thermostability of PDE4A11

Soluble (S2) and particulate (P) fractions of PDE4A11 were incubated for the indicated times at 55˚C prior to assay of their cAMP PDE activity with 1μM cAMP as substrate. The log % residual activity is plotted here as a function of time with the half life determined as that time where 50% of the activity remained. Data are from three separate experiments with means ± SD shown here.

Figure 9. PDE4A11 is phosphorylated by Protein Kinase A (PKA).

(a) COS7 cells transfected to express PDE4A11 are challenged with forskolin (100μM) together with IBMX (100μM). At the indicated times cells were harvested and lysates analysed by western blotting using an antisera specific for the phosphorylated form of UCR1, within the motif RRES(Phospho)W. A 126kDa single immunoreactive band was identified in a time dependent fashion (upper panel). The lower panel shows the result of western blotting these fractions with a pan PDE4A antiserum so as to provide

Molecular Pharmacology Fast Forward. Published on February 28, 2005 as DOI: 10.1124/mol.104.009423
This article has not been copyedited and formatted. The final version may differ from this version.

loading controls. (b) shows the dose-dependent inhibitory effect that the PKA inhibitor, H89 exerts on this process, with blotting in the upper panel showing data for the phospho-UCR1 antiserum with an arrow indicating the expected position for PDE4A11 and the lower panel providing the loading control done with a PDE4A antiserum. (c) shows the effect of treating cells transfected with the Ser119Ala mutant form of PDE4A11 with forskolin (100μM) together with IBMX (100μM) for the indicated times prior to immunoblotting as above with these two antisera. (d) shows the effect of treating COS7 cells transfected to express PDE4A11 for the indicated times with forskolin (100μM) together with IBMX (100μM) on the lysate PDE4A11 activity for 3 separate experiments with data as means ± SD. (e) shows the densitometric quantification of the labelling of P-UCR1 in COS7 cells transfected to express PDE4A11 and challenged with forskolin (100μM) together with IBMX (100μM) with lysates analysed at the indicated times cells, as in fig 10a, but for 3 separate experiments with data as means ± SD

Figure 10. Evaluation of LYN SH3, caspase-3 and βarrestin2 on PDE4A11.

(a) Shows pull-down assays to probe the interaction between the indicated PDE4A isoforms and the purified SH3 domain of LYN expressed as a GST fusion protein. 'B' indicates the GST-(LYN SH3 domain) fraction bound to glutathione agarose beads and 'U' indicates the unbound fraction from the pull-down experiment. This analysis was done exactly as described before by us for PDE4A11 and PDE4A4 (McPhee et al., 1999; Rena et al., 2001), with equal levels of input of each PDE4A species, as assessed immunologically using the C-terminal PDE4A specific antiserum. Thus the level of pull-down achieved by GST-LYN SH3 can be compared for the indicated 3 long PDE4A isoforms, with visualization done using the PDE4A specific antiserum in western blots. The control is a bead pull-down done using GST alone and with PDE4A11 present; similar null pull-down was achieved with PDE4A4 and PDE4A10 in the presence of GST as described previously (McPhee et al., 1999; Rena et al., 2001).

(b) Shows the effect of incubating the indicated PDE4A long isoform with activated caspase-3. Equal immunoreactive amounts of the indicated PDE4A isoforms were incubated with the same amount of activated caspase-3 (see Methods) prior to

analysis by western blotting with an antibody directed to the common C-terminal region of PDE4A. The panels indicate the only immunoreactive species apparent and the gels are typical of ones done at least 3 times. PDE4A10 and PDE4A11 were identified as single bands whose migration and intensity was unaffected by caspase-3 treatment (around 126kDa). Untreated PDE4A4 migrated at 127kDa, however, caspase-3 treatment caused the appearance of a novel 120kDa species detected by the pan-PDE4A (C-terminal) antisera, but which was not seen with the PDE4A4 specific (N-terminal) antiserum. Also shown is the action of caspase-3 on the rodent PDE4A4 homologue, PDE4A5.

(c) Shows pull-down assays to probe the interaction between the indicated PDE4A isoforms and the purified GST fusion protein of βarrestin, as described before (Baillie et al., 2003; Bolger et al., 2003; Perry et al., 2002). Descriptions are as in section (a) above.

All these data are typical of experiments done three times with different transfections.

Acc. No.	species	4A4B	4A11	4A10	exon 2	exon 3	exon 4	exon 5	exon 6	exon 7	exon 8
BF346277	human	yes			yes	yes	yes	x	x	x	x
BY015160	mouse	yes			x	x	x	x	x	x	x
BY124416	mouse	yes			x	x	x	x	x	x	x
CA775139	human		yes		yes	yes	yes	yes	yes	yes	yes
AW104482	human		yes		yes	yes	yes	yes	yes	x	x
CA774868	human		yes		yes	yes	yes	yes	yes	yes	x
BI438716	human		yes		yes	yes	yes	yes	x	x	x
BF732322	human		yes		x	x	x	x	x	x	x
BF116176	human		yes		x	x	x	x	x	x	x
AW296744	human		yes		x	x	x	x	x	x	x
BI156706	mouse		yes		yes	x	x	x	x	x	x
BY352528	mouse		yes		yes	x	x	x	x	x	x
BY184004	mouse		yes		yes	x	x	x	x	x	x
BY183996	mouse		yes		yes	x	x	x	x	x	x
BY353288	mouse		yes		yes	x	x	x	x	x	x
BY209230	mouse		yes		yes	x	x	x	x	x	x
BY352150	mouse		yes		yes	x	x	x	x	x	x
BY347207	mouse		yes		yes	x	x	x	x	x	x
BX921915	pig		yes		yes	x	x	x	x	x	x
BF300255	mouse			yes	yes	yes	yes	yes	yes	x	x
CK795128	mouse			yes	yes	x	x	x	x	x	x
BY748490	mouse			yes	yes	x	x	x	x	x	x
BY749598	mouse			yes	yes	x	x	x	x	x	x
BE531640	mouse			yes	yes	x	x	x	x	x	x
CK482793	rat			yes	yes	x	x	x	x	x	x

Table 1. The bio-informatic identification and analysis of PDE4A11 ESTs from various species

Shown are the GenBank descriptors for ESTs that encode either PDE4A11 or PDE4A4B or PDE4A10 by virtue of their having the appropriate exon-1 sequence. Also shown is whether such ESTs have sequence representing *PDE4A* downstream exons. The

largest of these ESTs for PDE4A11 extends from exon-1 down to exon-8, which lies in the PDE4A catalytic unit (CA775139).

Molecular Pharmacology Fast Forward. Published on February 28, 2005 as DOI: 10.1124/mol.104.009423
This article has not been copyedited and formatted. The final version may differ from this version.

Table 2 Inhibition of PDE4A11 by PDE4 family selective inhibitors.

Assays were done with 1μM cAMP as substrate using the range and number of inhibitor concentrations as indicated in Fig 8. By far the major fraction of PDE4A10 is soluble in lysed cells and thus data is only provided for the S2 fraction. The data reflect the average of three separate experiments with IC_{50} values given as the mean ± SD in μM.

Inhibitor	**PDE4A11 (S2)**	**PDE4A11 (P2)**	**PDE4A4B (S2)**	**PDE4A4B (P2)**	**PDE4A10 (S2)**
Rolipram	0.72 ± 0.08	0.66 ± 0.12	1.31 ± 0.08	0.26 ± 0.09	0.064 ± 0.009
Ariflo (cilomilast)	0.034 ± 0.005	0.034 ± 0.005	0.061 +/- 0.007	0.059 +/- 0.004	0.13 ± 0.03
Roflumilast	0.0048 ± 0.0004	0.0039 ± 0.0002	0.0090 +/- 0.0016	0.0025 +/- 0.0009	0.0041 ± 0.0008
Denbufylline	0.25 ± 0.06	0.31 ± 0.04	0.56 +/- 0.30	0.46 +/- 0.20	0.59 ± 0.17
Ro 20-1724	0.99 ± 0.11	0.91 ± 0.07	2.93 +/- 1.16	2.90 +/- 0.10	1.24 ± 0.07

Molecular Pharmacology Fast Forward. Published on February 28, 2005 as DOI: 10.1124/mol.104.009423
This article has not been copyedited and formatted. The final version may differ from this version.

Table 3. Summary of PDE4A11 distinguishing features.

Property	**Comment**
Rolipram inhibition	Unlike 4A4, particulate and soluble forms of 4A11 show no difference in sensitivity to inhibition by rolipram.
Chronic rolipram treatment.	Unlike 4A4, chronic treatment of cells with rolipram does not cause redistribution of 4A11 within cells.
Ro20-1724	4A11 and 4A10 are more potently inhibited than 4A4
Roflumilast	Unlike 4A4, soluble and particulate 4A11 forms show similar sensitivity to inhibition by roflumilast.
Denbufylline	4A11 is more sensitive to inhibition than 4A4 or 4A10
Ariflo (cilomilast)	4A10 is less sensitive to inhibition than 4A4 or 4A11
Distribution	Unlike 4A4 and 4A11, 4A11 is found in plasma membrane ruffles.
LYN (SH3 domain)	4A11 and 4A10 show a lower propensity of associating with LYN through its SH3 domain than does 4A4
Thermal stability of soluble 4A11	Soluble 4A11 is dramatically more thermolabile than the soluble form of other PDE4A long isoforms.
Thermal stability of particulate 4A11	Particulate 4A11 is more thermolabile than 4A4 but similarly thermolabile to 4A10
Comparative thermostability of soluble and particulate forms	Whilst particulate 4A11 is more thermostable than cytosolic 4A11 the converse is true for both 4A10 and 4A4.
Caspase-3	Only PDE4A4 is cleaved by caspase-3
βarrestin2	All 3 isoforms can interact with βarrestin2
PKA phosphorylation	Similar to other PDE4A long isoforms
Km cAMP	Similar to other PDE4A long isoforms
Vmax cAMP hydrolysis	Similar to other PDE4A long isoforms

Fig 1a

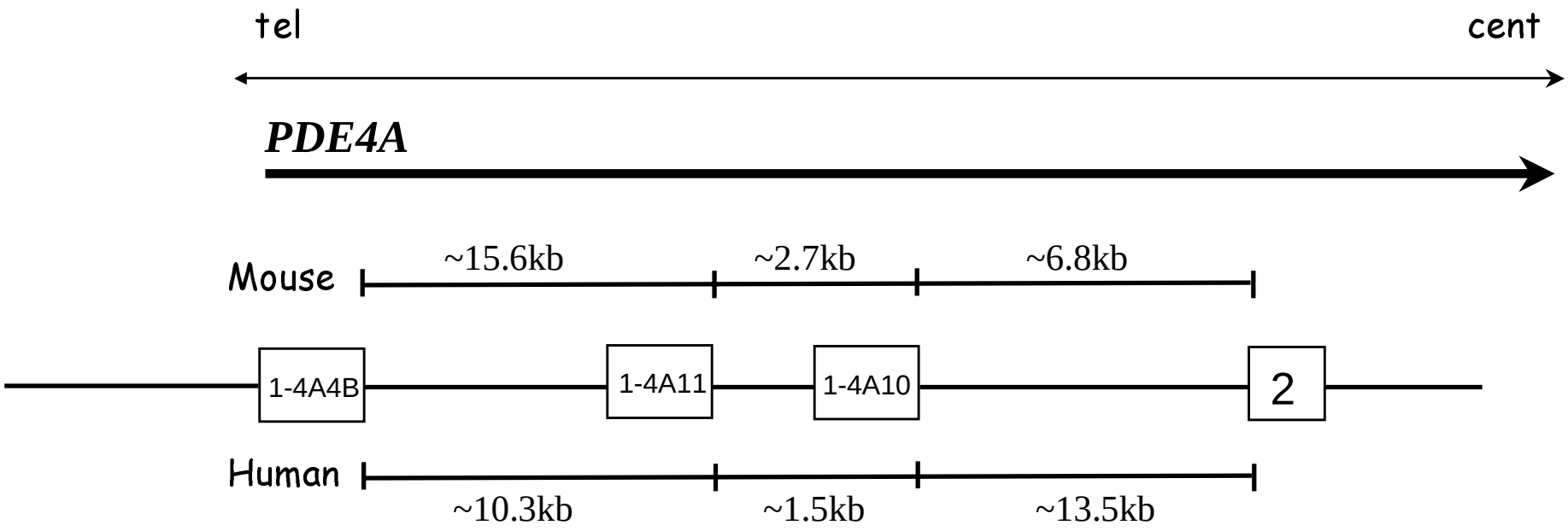

Fig 1b

T*GTCCCCACAGATTTGGG**GTGTCCCTGGTGTTTGTGGGGACGCGTCCGGCGATTGTGAG**GAC*

*ATTAGAGCCAACGCGGGCGGCTTTGGGGTCTGCGGGAGAGTCCCCACCAGAGCCGTGC**GGGCG***

*CCCCAGACCCGCCCCGCCCTGGGGGCGGCTCCAGCGCGAAGCCGGAAGGGCCGAGGC**GACAGG***

*GCGGGGTGGGGCCCGCGGGCCCGGGGCTGGGCAGGCGGCCTGCGTGGGCCTGGCGG**GGTGGGC***

Exon 1-4A11

METAlaArgProArgGly

GGCGCAGCTCCCCAGCGCCCGCCGAGGCGGGGCCGCCCCGAGC**ATGGCGCGGCCGCGC**GGC

LeuGlyArgIleProGluLeuGlnLeuValAlaPheProValAlaValAlaAlaGluAspGlu

CTAGGCCGCATCCCGGAGCTGCAACTGGTGGCCTTCCCGGTGGCGGTGGCGGCTGAGGACGAG

AlaPheLeuProGluProLeuAlaProArgAlaProArgArgProArgSerProProSerSer

GCGTTCCTGCCCGAGCCCCTGGCCCCGCGCGCGCCCCGCCGCCCGCGTTCGCCGCCCTCCTCG

ProValPhePheAlaSerProSerProThrPheArgArgArgLeuArgLeuLeuArgSerCys

CCCGTCTTCTTCGCCAGCCCGTCCCCAACTTTCCGCAGACGCCTTCGGCTTCTCCGCAGCTGC

GlnAspLeuGlyArgGlnAlaTrpAlaGlyAlaGl

CAGGATTTGGGCCGCCAGGCTTGGGCGGCTGGgaagtgcagcgc…….. 15kb…….

Exon 2

yPheGluAlaGluAsnGlyProThrPro

…….tcccctgcagCTTCGAGGCAGAGAATGGGCCGACACCA

Fig 2a

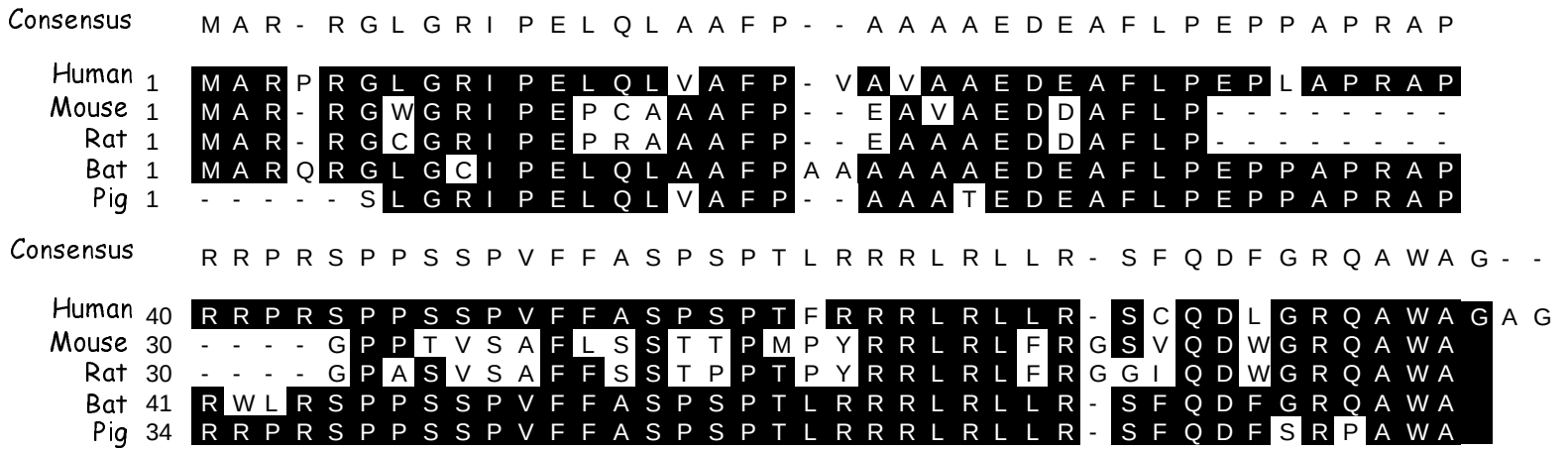

Fig 2b

Murine 3′ splice	AG/GCT/TGG/GCC/GGgtgagtgcgc
Rat 3′ splice	AG/GCG/TGG/GCT/Gggtgagtgtgc
Bat 3′ splice	AG/GCG/TGG/GCC/GGgtaagtgcgc

Fig 3a

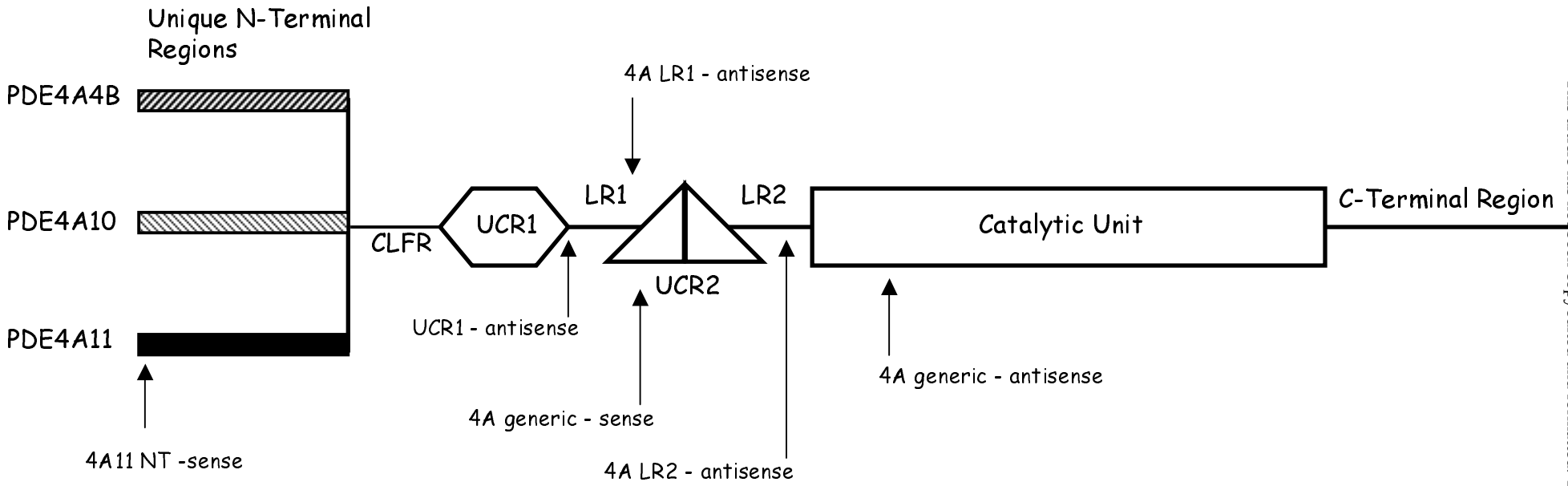

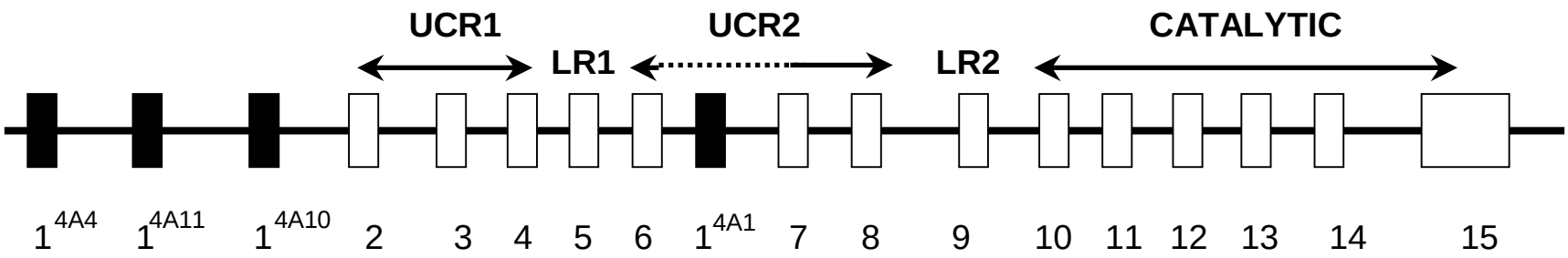

Fig 3b

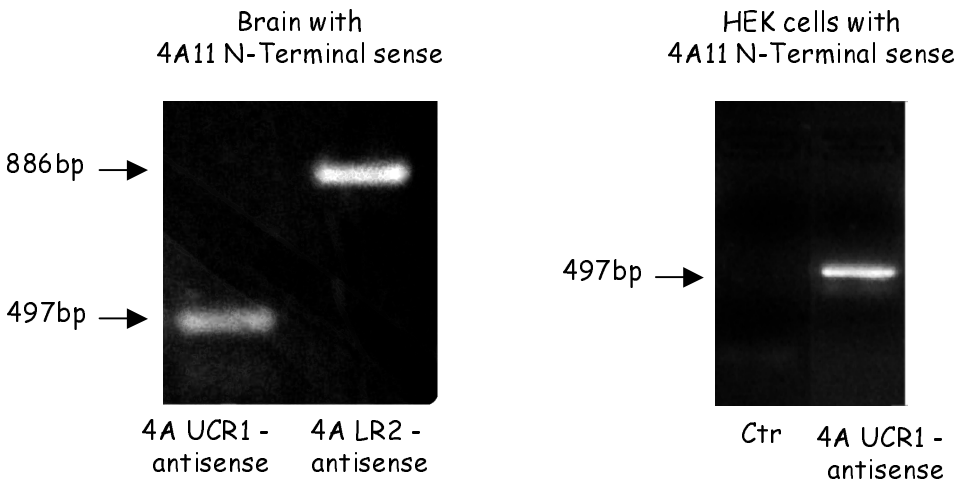

Fig 4a

Fig 4b

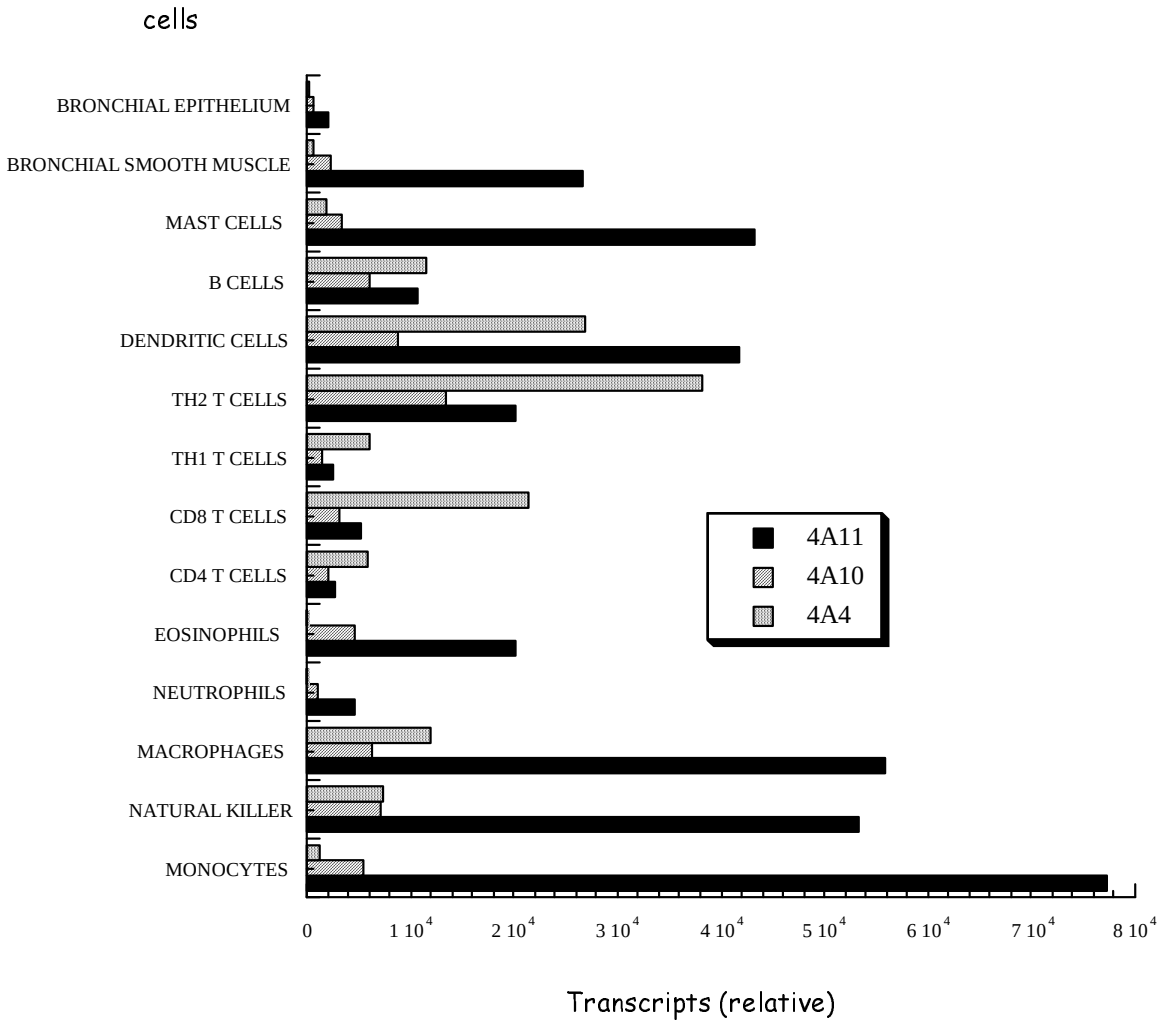

Fig 5ab

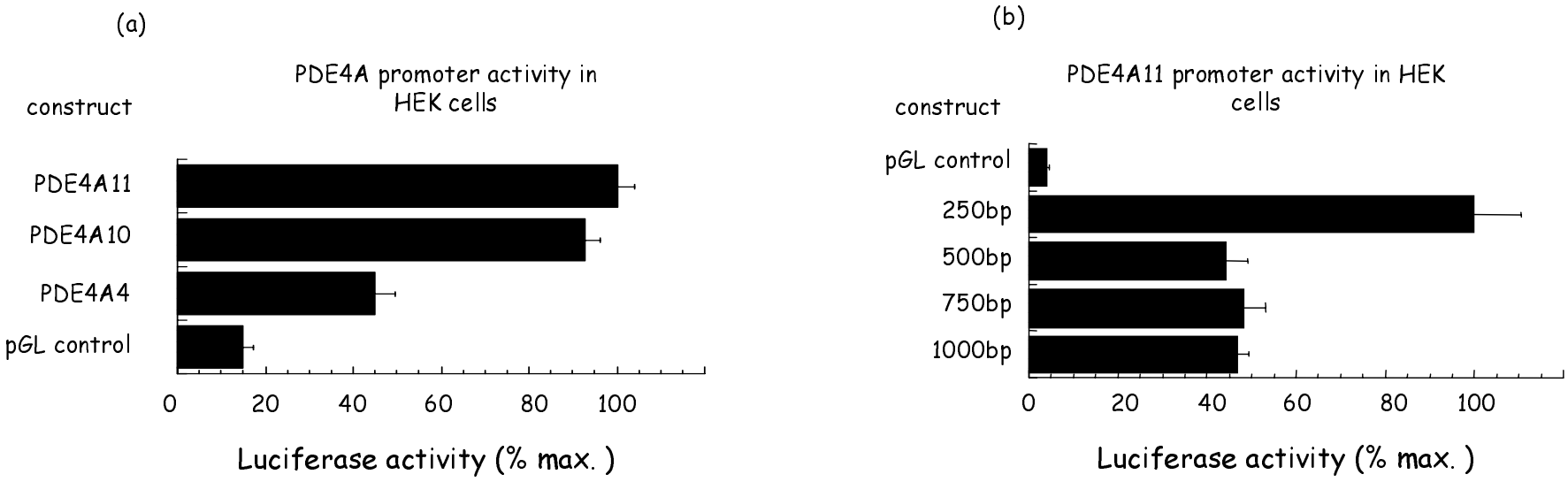

Fig 5c

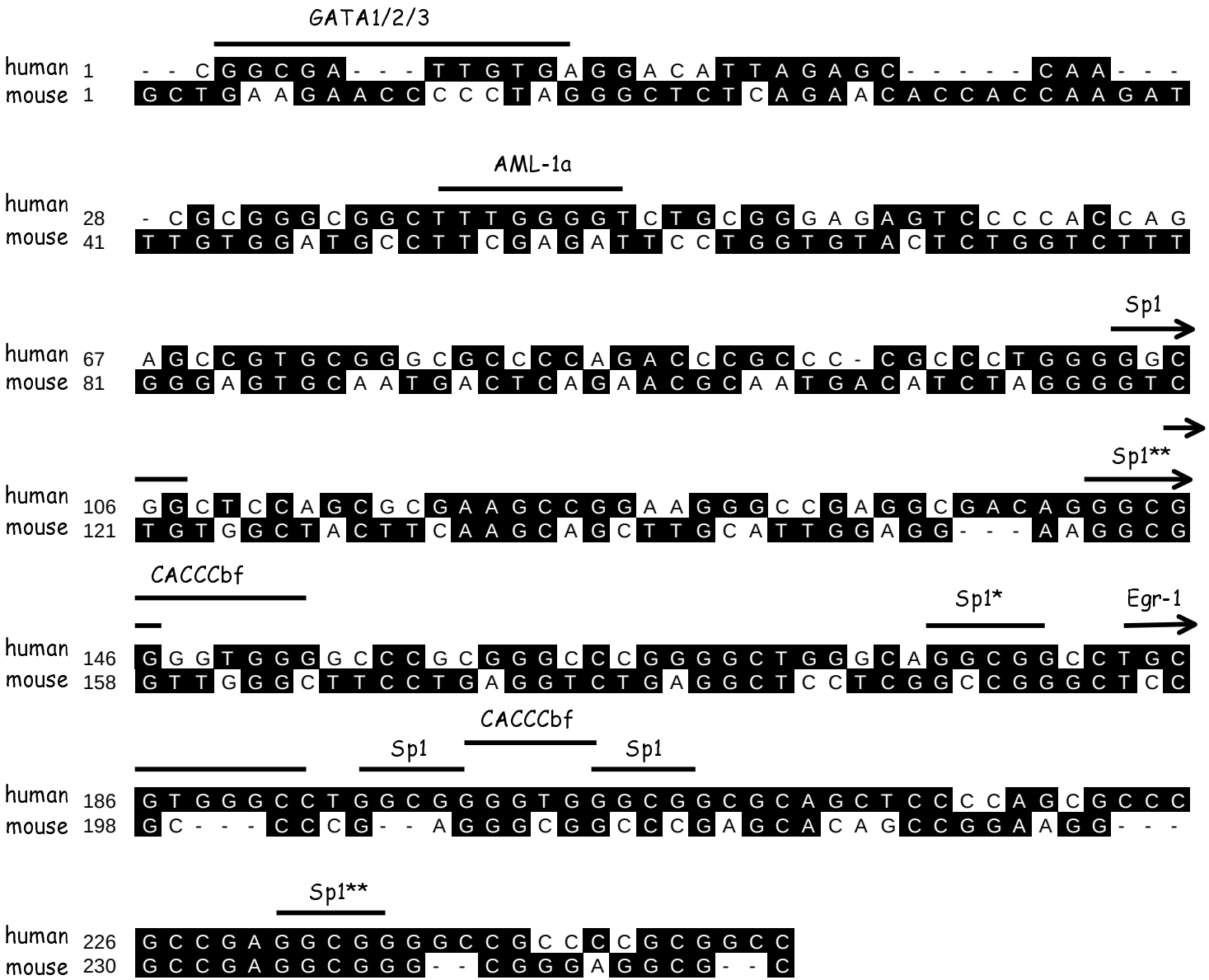

Fig 6ab

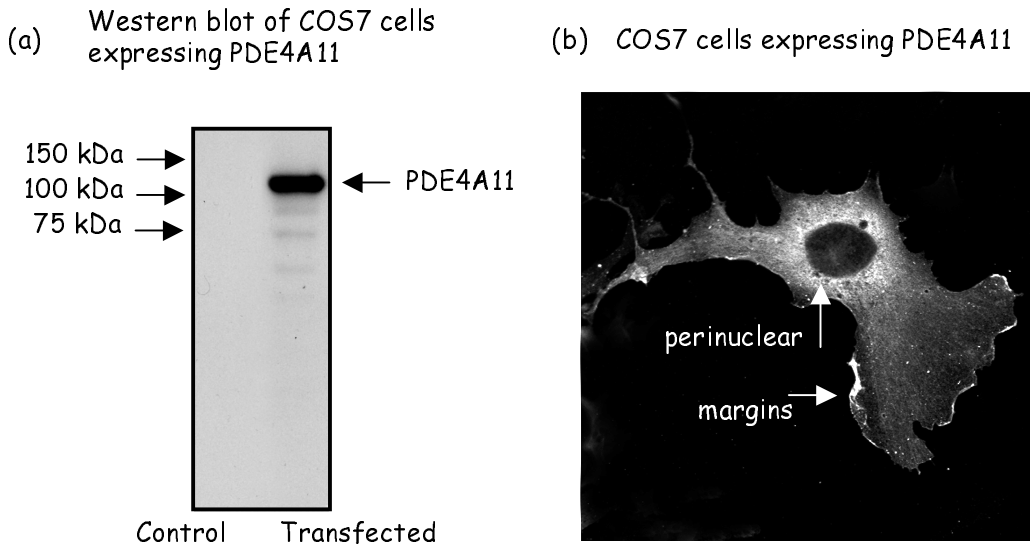

Fig 6c

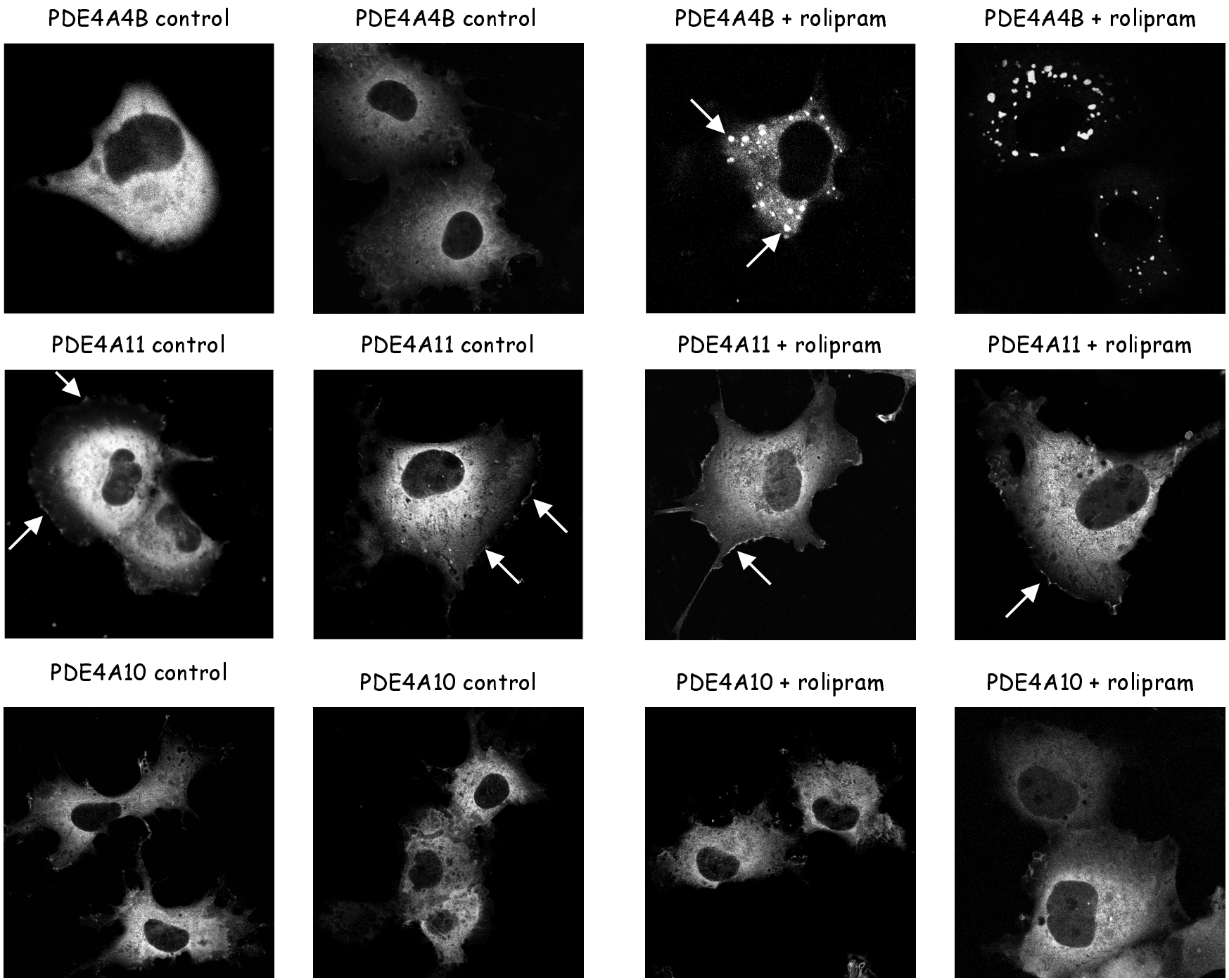

Fig 7

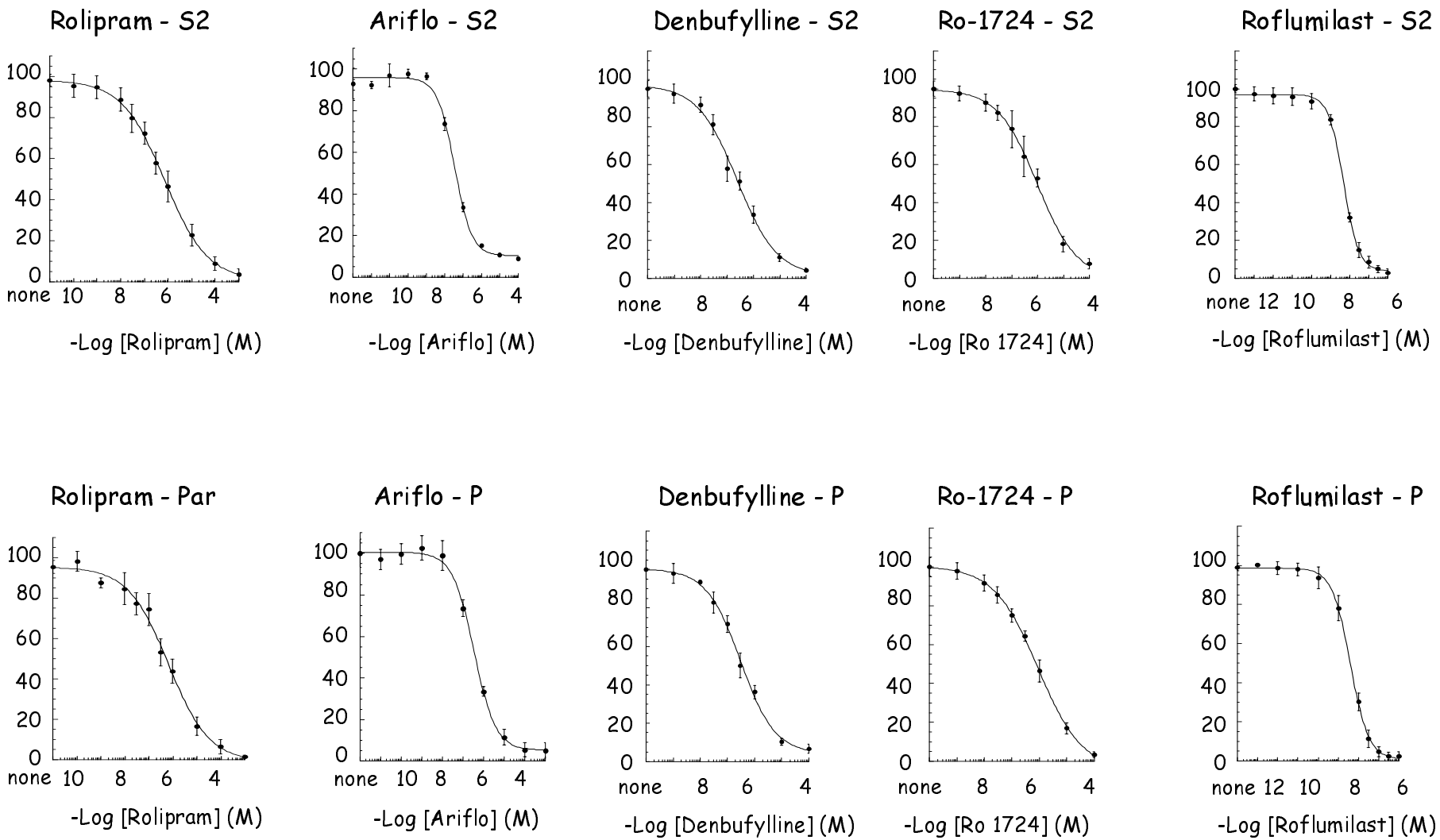

Fig 8

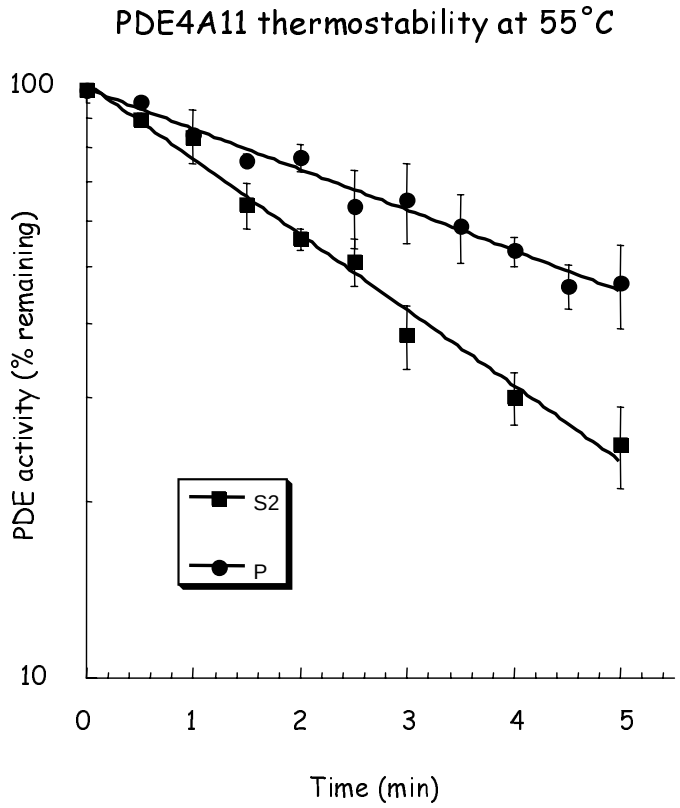

Fig 9abc

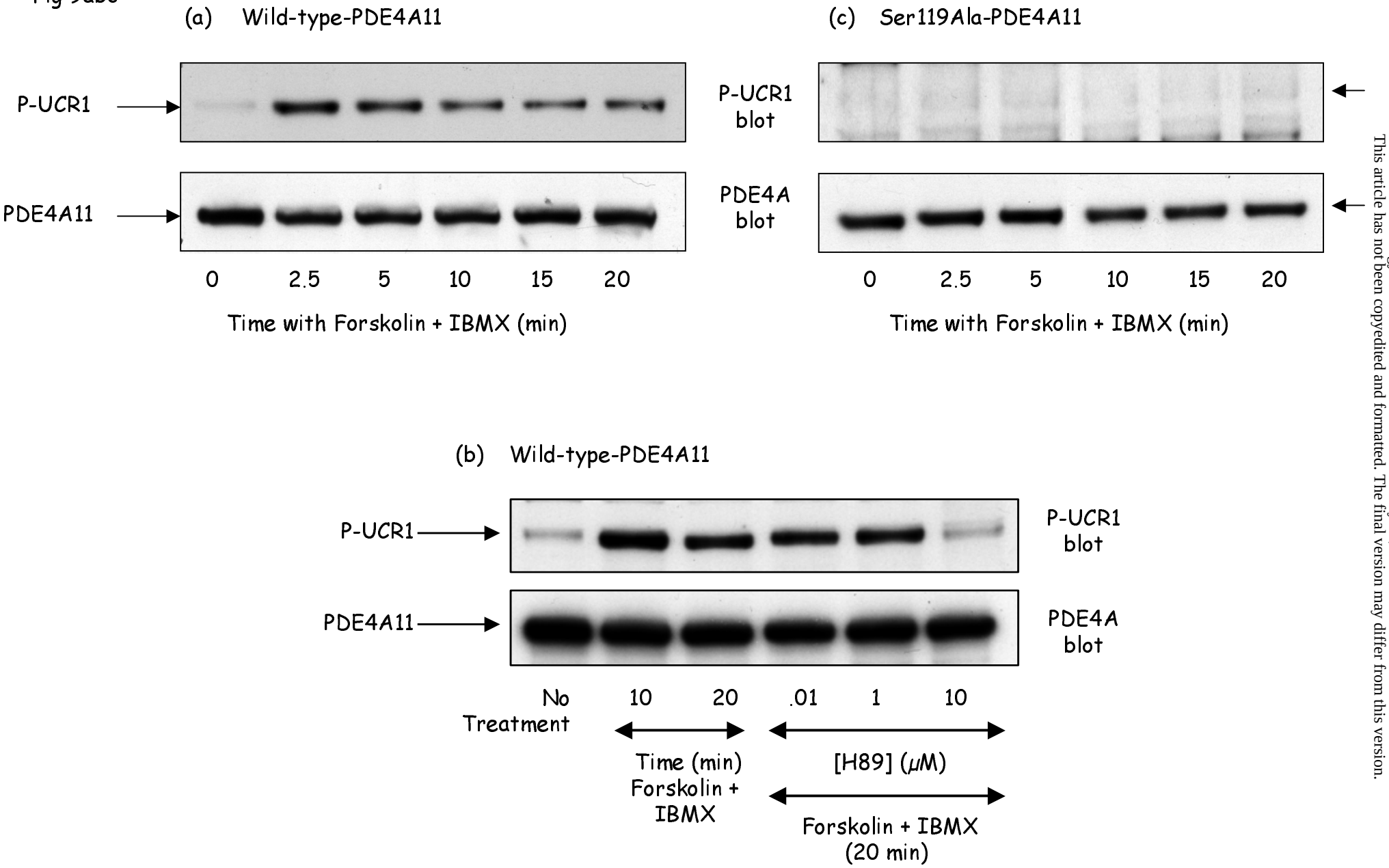

Fig 9de

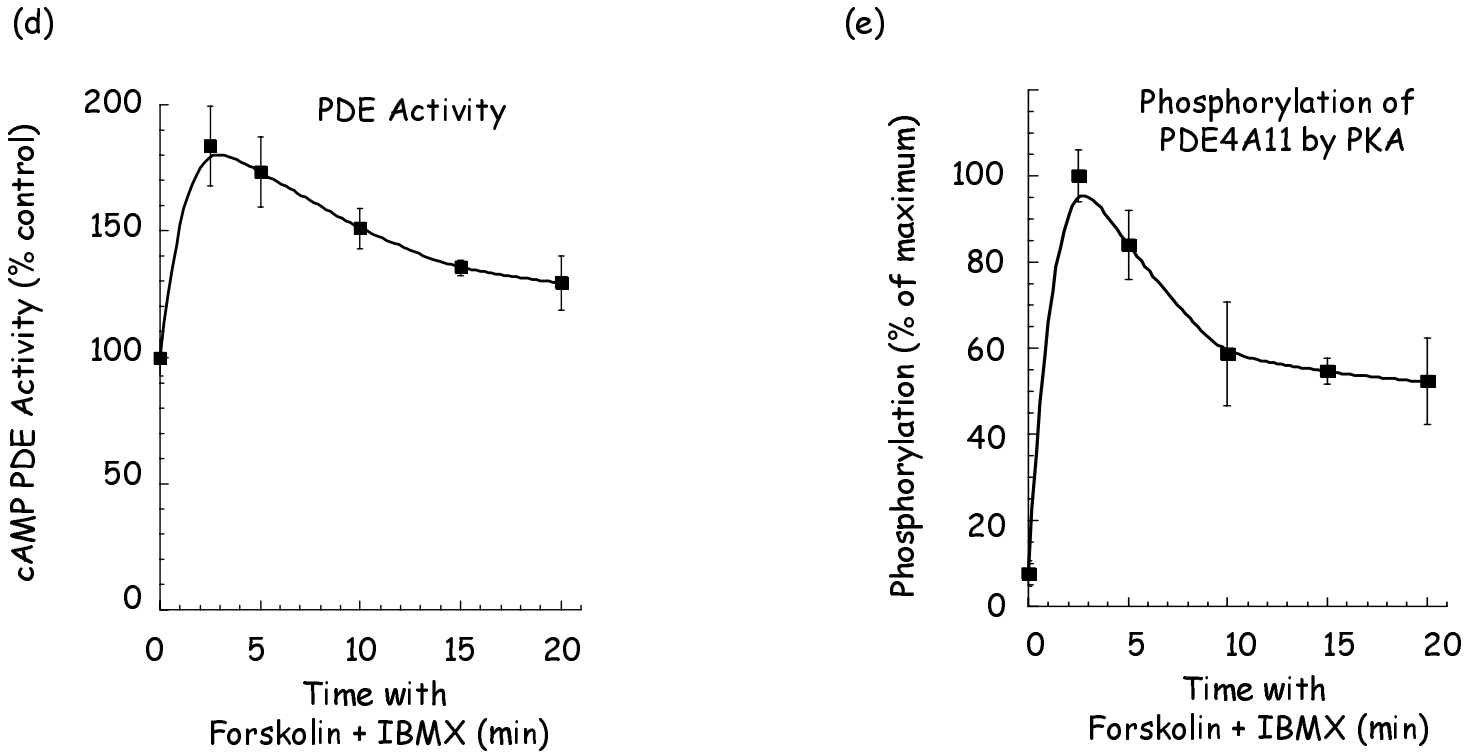

Molecular Pharmacology Fast Forward. Published on February 28, 2005 as DOI: 10.1124/mol.104.009423
This article has not been copyedited and formatted. The final version may differ from this version.

Fig 10